INCREASING WELL PRODUCTIVITY IN GAS CONDENSATE WELLS IN QATAR'S NORTH FIELD

A Thesis

by

NATHAN MILLER

Submitted to the Office of Graduate Studies of
Texas A&M University
in partial fulfillment of the requirements for the degree of

MASTER OF SCIENCE

December 2009

Major Subject: Petroleum Engineering

INCREASING WELL PRODUCTIVITY IN GAS CONDENSATE WELLS IN QATAR'S NORTH FIELD

A Thesis

by

NATHAN MILLER

Submitted to the Office of Graduate Studies of
Texas A&M University
in partial fulfillment of the requirements for the degree of

MASTER OF SCIENCE

Approved by:

Chair of Committee,	Ding Zhu
Committee Members,	Hadi Nasrabadi
	Maria Barrufet
	Akhil Datta-Gupta
Head of Department,	Steve Holditch

December 2009

Major Subject: Petroleum Engineering

ABSTRACT

Increasing Well Productivity in Gas Condensate Wells in Qatar's North Field.

(December 2009)

Nathan Miller, B.S., Texas A&M University

Chair of Advisory Committee: Dr. Ding Zhu

Condensate blockage negatively impacts large natural gas condensate reservoirs all over the world; examples include Arun Field in Indonesia, Karachaganak Field in Kazakhstan, Cupiagua Field in Colombia, Shtokmanovskoye Field in Russian Barents Sea, and North Field in Qatar. The main focus of this thesis is to evaluate condensate blockage problems in the North Field, Qatar, and then to propose solutions to increase well productivity in these gas condensate wells. The first step of the study involved gathering North Field reservoir data from previously published papers. A commercial simulator was then used to carry out numerical reservoir simulation of fluid flow in the North Field. Once an accurate model was obtained, the following three solutions to increasing productivity in the North Field are presented: namely wettability alteration, horizontal wells, and reduced Non Darcy flow.

Results of this study show that wettability alteration can increase well productivity in the North Field by adding significant value to a single well. Horizontal wells can successfully increase well productivity in the North Field because they have a smaller pressure drawdown (compared to vertical wells). Horizontal wells delay

condensate formation and increase the well productivity index by reducing condensate blockage in the near wellbore region. Non Darcy flow effects were found to be negligible in multilateral wells due to a decrease in fluid velocity. Therefore, drilling multilateral wells decreases gas velocity around the wellbore, decreases Non Darcy flow effects to a negligible level, and increases well productivity in the North Field.

DEDICATION

"So whether you eat or drink or whatever you do, do it all for the glory of God."

1 Corinthians 10:31 (NIV)

ACKNOWLEDGEMENTS

I would like to thank my committee chair, Dr. Zhu, for allowing me to join QNRF ID 590 “Using Horizontal and Multilateral Well with Intelligent Completion to Develop Gas Fields in Qatar.” I would like to thank Dr. Nasrabadi for being my direct supervisor for the last 12 months I have spent living in Qatar. I have enjoyed having a chance to study under your supervision. Most of all, I am grateful for the partnership between Texas A&M University and Qatar Foundation. Your partnership has allowed me to travel the world, observe new cultures, practice new languages, and play basketball for Texas A&M Qatar.

TABLE OF CONTENTS

Page

Page

LIST OF FIGURES

FIGURE Page

LIST OF TABLES

1. INTRODUCTION

1.1. Background

Natural gas is a nonrenewable energy source that is mainly used for heating and generating electricity. The price of natural gas depends on production, imports, demand, current inventory, and oil price. Between 300 and 400 million years ago, plant and animal remains decayed and built up into large layers. Over millions of years, this organic material became trapped between rock, where pressure and heat changed the organic material into coal, oil, and small bubbles of natural gas. Natural gas is an odorless gas composed mainly of methane, or one carbon atom and four hydrogen atoms (Energy Information Administration, 2009). As seen from Fig. 1, the natural gas industry can be divided into 3 stages: production, transmission, and distribution.

This thesis follows the style of *SPE Reservoir Evaluation & Engineering*.

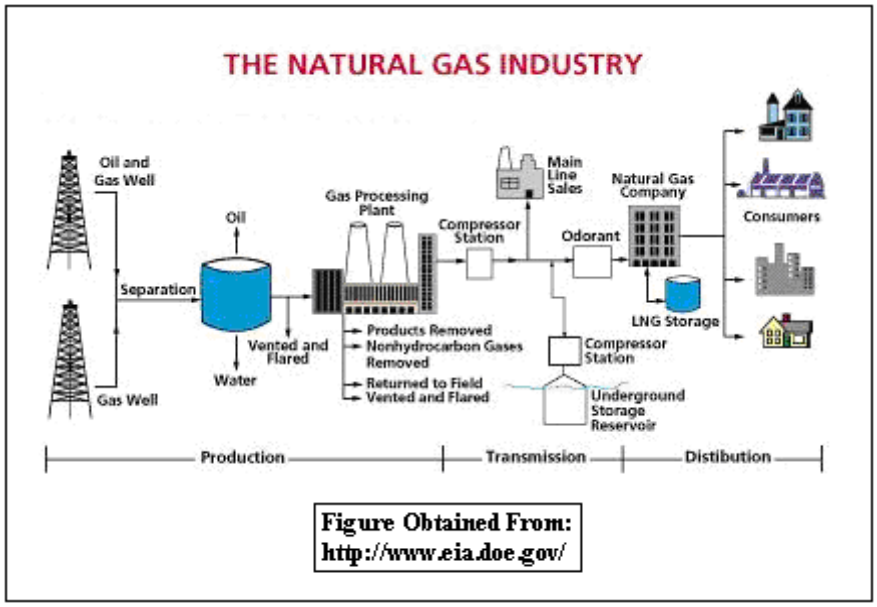

Fig. 1: The Natural Gas Production and Distribution Chain

During the production stage, gas is taken out of the ground and sent to a separator which removes oil and water. The gas can then be flared or sent to a gas processing plant to remove non-hydrocarbon gases. The next step involves the transmission stage where the gas is sent to a compressor station, and then either stored underground, delivered to a main sales line, or transferred to a natural gas company. In some cases natural gas must travel long distances to reach a consumer market. In these instances, pipelines are not sufficient in transporting natural gas from the wellhead to the consumer, and two other options become economical: liquefied natural gas (LNG) and gas-to-liquids (GTL). LNG is natural gas that has been converted temporarily to liquid form and takes up 1/600th the volume of natural gas (Energy Information Administration, 2009). The liquefication process includes removing components like dust, helium, water, and heavy

hydrocarbons, and then physically turning the gas into liquid by cooling it to –260 ºF (Energy Information Administration, 2009). GTL involves chemically converting natural gas into longer-chain hydrocarbons which involves the following three steps: production of synthesis gas, conversion of the synthesis gas to waxy hydrocarbon material, and hydrocracking the waxy material to the desired products (Rahman and Al-Maslamani 2004). The distribution stage begins once the gas is sent to the natural gas company, which can either store the gas as liquefied natural gas, or deliver the final product to the consumer. In 2008, 23 Tcf of natural gas was consumed in the United States in the following manner (Energy Information Administration, 2009):

- 29% Industrial
- 29% Electrical power generation
- 21% Residential
- 13% Commercial
- 6% Lease and plant fuel consumption
- 2.7% Pipeline and distribution
- 1% Vehicle fuel

Natural gas is measured and sold in British Thermal Units (Btu). A Btu is the heat required to raise the temperature of one pound of water one degree Fahrenheit.

1.2. Future Importance of Natural Gas

Natural gas will continue to play an important part of the future economy because of three reasons. First, there are a lot of natural gas reserves in the world. Fig. 2 shows world natural gas reserves and their location. At current natural gas consumption levels, it would take over 40 years to exhaust natural gas reserves globally.

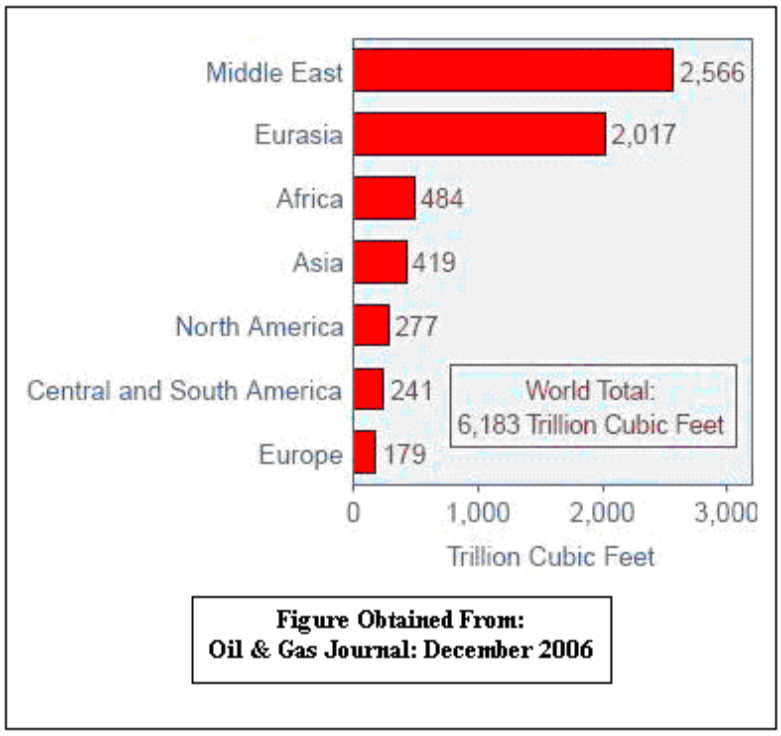

Fig. 2: Natural Gas Reserves Worldwide

Second, the worldwide consumption of natural gas is expected to increase dramatically over the next few decades. The Energy Information Administration expects natural gas consumption to increase worldwide from 104 trillion cubic feet in 2005 to 158 trillion cubic feet in 2030 (Energy Information Administration, 2009). Third, natural gas is more environmentally friendly than other fossil fuels because it burns cleaner. Natural gas emits less sulfur, carbon, and nitrogen than coal or oil, and it leaves smaller amounts of ash particles when burned.

1.3. Phase Behavior of Reservoir Fluids

There are five categories of reservoir fluids: black oil, volatile oil, retrograde gas, wet gas, and dry gas. The type of fluid found in a reservoir can only be verified in the laboratory, however, there are some property guidelines that can help identify the fluid category in the field. The initial producing gas-oil ratio, the gravity of the stock-tank liquid, and the color of the stock-tank liquid are three fluid properties that can be used in the field to determine what type of fluid is in a reservoir. Retrograde gases exhibit a lower GOR limit of 3300 scf/stb and an upper GOR limit of 150,000 scf/stb. Retrograde gases have stock-tank liquid gravities between 40° and 60° API, and can be lightly colored, orange, brown, greenish, or water-white in color. This thesis focuses on the North Field, which is a retrograde gas reservoir. Retrograde gases are referred to as retrograde gas-condensates, retrograde condensate gases, gas condensates, and condensates. However, the most accurate name is retrograde gas since the fluid in the reservoir is initially a gas fluid exhibiting retrograde behavior (McCain 1990). Fig. 3 shows a phase diagram of a retrograde gas, and a saturation envelope which looks like an enclosed pouch. A fluid outside the saturation envelope is in single phase (liquid **or** gas), and a fluid inside the saturation envelope is in two-phase (liquid **and** gas). In order to understand Fig. 3, a few terms need to be defined. The bubble point is the point at which the first molecules leave the liquid state and form a small bubble of gas. The bubble point line in a phase diagram represents the bubble point over a range of temperature and pressure changes. The dew point is the point at which the first molecules leave the gas state and form liquid. The dew point line in a phase diagram

represents the dew point over a range of temperature and pressure changes. The critical point is where the bubble-point line and dew-point line meet, and represents the point at which all the properties of liquid and gas become similar. The cricondentherm is the highest temperature on the saturation envelope. Fig. 3 shows that for a retrograde gas, the critical temperature is less than the reservoir temperature while the cricondentherm is greater than the reservoir temperature.

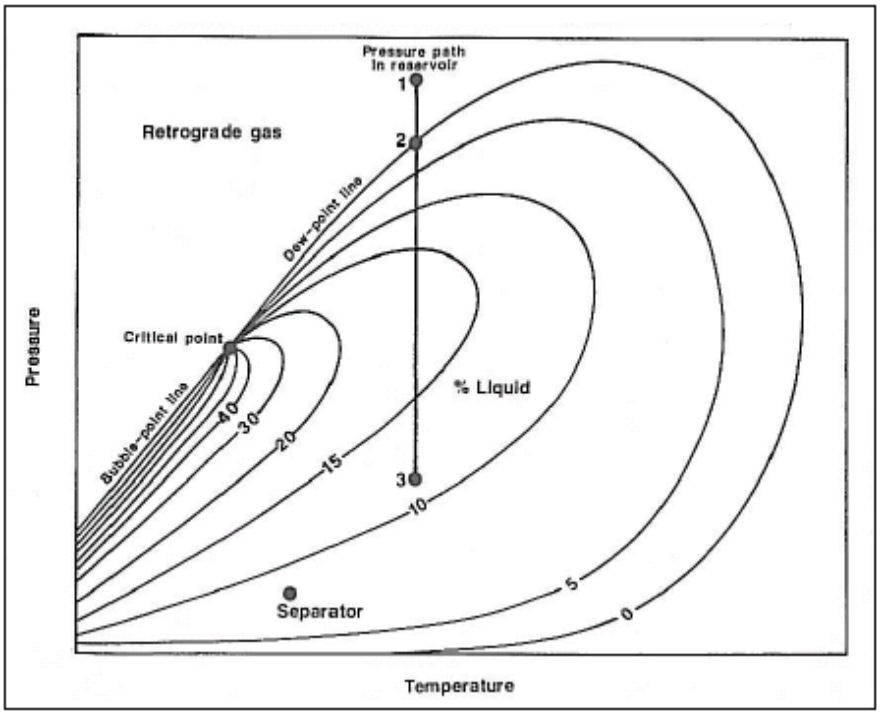

Fig. 3: Phase Diagram

1.4. Significance of Gas Condensate in Gas Production

Much of the 6,183 trillion cubic feet of worldwide gas reserves can be found in gas-condensate reservoirs. For this reason gas condensate reservoirs are important to understand. Some of the largest gas-condensate reservoirs in the world include the Arun Field in Indonesia, the Cupiagua Field in Colombia, the Karachaganak Field in Kazakhstan, the North Field in Qatar which borders with the South Pars Field in Iran, and the Shtokmanovskoye Field in the Russian Barents Sea (which has very little published data). All of these large gas condensate fields have one thing in common: condensate blockage. Condensate blockage occurs due to fluid phase properties, formation flow characteristics, and pressures in the formation and in the wellbore. Production performance can decrease dramatically if these condensate banking effects are not understood at the start of field development.

1.4.1. The Arun Field

The Arun Field is located on the northern coast of Aceh Province in North Sumatra, Indonesia. The Arun reservoir had an initial gas in place of 16.8 TCF of dry gas and an initial condensate in place of 840 million barrels. The ultimate recovery is expected to be 94% of the initial gas in place and 87% of the initial condensate in place, which ranks as one of the highest recoveries worldwide for a gas condensate field (Pathak *et al*. 2004). The reservoir consists of dense limestone up to 1,000 ft in thickness and covers an area of 23,000 acres. However, after 10 years of production, significant productivity loss was due to condensate accumulation in the near wellbore region (Afidick *et al*. 1984).

1.4.2. The Cupiagua Field

The Cupiagua Field is another example of a large gas condensate reservoir that experiences the negative effects of condensate blockage. The Cupiagua Field is a large gas condensate reservoir that lies in the Llano Basin in Colombia. It has a communicating vertical thickness of about 5,000 ft, it has an average surface condensate yield of 300 stb/mmscf, and most of its hydrocarbons exists at a near critical condensate state. Since most of its hydrocarbons exists at near critical conditions, condensate accumulation will start forming fairly quickly after the reservoir pressure drops below the dew point pressure (Lee and Chaverra 1998).

1.4.3. The Karachaganak Field

The Karachaganak Field is a large near-critical gas condensate reservoir located in northwest Kazakhstan close to the Russian border. The field contains a gas column 4,757 ft in height with 42.4 Tcf of gas in place (Elliott *et al*. 1998). The initial reservoir pressure and temperature ranges are 520 to 595 bar and 70 to 95 degrees Celsius. The reservoir contains a complex gas condensate fluid system with a fluid that ranges from a rich gas condensate of 2,000 scm/scm at the reservoir top to 800 scm/scm at the GOC (Al-Shammasi and D'Ambrosio 2003).

1.4.4. The North Field

Qatar's North Field will be the focus of this thesis since the reservoir simulator used in this study is built off North Field fluid and geologic data. The North Field is a massive offshore gas-condensate reservoir that holds more than 900 TCF of proven natural gas reserves, which makes it the largest non-associated gas field in the world.

The abnormally pressured field covers over 6,000 square kilometers. The North Field extends into Iran's South Pars Field which has 280 Tcf of recoverable natural gas reserves (Energy Information Administration, 2009). The initial reservoir pressure is 5,300 psi, and the initial reservoir temperature is 220 degrees Fahrenheit. The field produces from a carbonate reservoir called the Khuff formation (late Permian to early Triassic age). The Khuff formation consists of four, non-communicating, highly stratified layers of carbonate: K1, K2, K3, and K4. The thickness of each unit is 204 ft, 327 ft, 255 ft, and 645 ft (Whitson and Kuntadi 2005). Limestone and dolomite with some interbedded shale, claystone, anhydrite, and sandstone make up the geology of the North Field. After the North Field was discovered in 1971, the next 14 years were spent drilling appraisal wells to quantify the reservoir gas accumulations, and determining the reservoir fluid and geological characteristics of the field (Benesch *et al*. 2007). The Alpha Project began in 1991 and was the first project to develop the field's reserves by producing natural gas and condensate from the Lower Khuff. The first concession was awarded in 1993, the first delivery of condensate occurred in 1996, and the first delivery of LNG took place in 1997. Since then, new LNG trains have been coming on every few years: two 3.25 MTPA LNG trains in 1999, three 4.7 MTPA LNG trains between 2004 and 2009, and two 7.8 MTPA LNG trains in 2009. Three types of well designs have been used to develop the North Field: the 5 inch by 5 and 1/2 inch completion tubing, the 7 inch monobore which handles flow rates up to 125 MMSCF/D, and the 7 and 5/8 inch by 9 and 5/8 inch OBB design which handles flow rates up to 200 MMSCF/D (Benesch *et al*. 2007).

1.5. Literature Review of Condensate Blockage and Solutions

Many experimental and numerical studies have been completed which show various ways to reduce condensate saturation around the wellbore. Some studies have focused on increasing viscous forces and decreasing interfacial tension, while others have focused on gas injection and decreasing liquid wetness. Ali *et al.* (1993) explored decreasing interfacial tension in order to reduce condensate saturation. They identified problem areas in condensate behavior, and proposed the need for coreflooding research and physical equilibrium property measurements. Ali et al. (1993) also showed how interfacial tension can influence liquid mobility in a gas condensate system for near critical fluids. They questioned the effect of IFT on liquid mobility, showed the potential of low-tension partial pressure maintenance as an efficient production technique, and found that gravity plays a strong effect on low-tension depletion. Boom *et al*. (1996) increased viscous forces to reduce condensate blockage near the wellbore. They used model experiments to study gas condensate mobility in the near-wellbore region, and found that both the wetting and nonwetting phase are significantly increased in the model experiments. They also found that the wetting phase relative permeability from the experiments can be incorporated into the field. Ahmed *et al*. (1998) analyzed gas injection methods as a solution to reducing condensate saturation around the wellbore. They studied the feasibility of reducing wellbore liquid blockage by the Huff ‘n’ Puff gas injection process, and found that the Huff ‘n’ Puff process is a feasible option for reducing the liquid blockage in the near wellbore region. Ahmed *et al*. (1998) also found that the process works best when it is initiated before maximum liquid

dropout. Li and Firoozabadi (June 2000) also experimented with increasing viscous forces in order to reduce condensate saturation. They used a phenomenological simple network model to study the effects of gravity, viscous forces, interfacial tension, wettability, and relative permeability of gas condensate systems. They found that wettability largely impacts both critical condensate saturation and relative permeability, and that the relative permeability may increase as the contact angle increases at certain saturations. Li and Firoozabadi (April 2000) tried decreasing liquid wetness in order to decrease condensate saturation in the near wellbore. They found that oil recovery and phase relative permeability in gas-oil systems could be increased by using FC-722 to alter the wettability of the matrix. They also found that the wettability of porous media can be changed permanently to gas-wetting.

1.6. Research Objectives

The first objective of this research is to better understand the negative impact condensate-blockage has on total gas production in gas condensate reservoirs. When condensate blockage occurs, it effects gas relative permeability. Previous work done by Narayanaswamy (1998) suggests Non Darcy effects tend to reduce the pressure and further produce more condensate dropout. The second objective of this research is to propose wettability alteration, horizontal wells, and Non Darcy flow reduction as three solutions for increasing well productivity in the North Field. Section 1 introduces background information on natural gas and gas condensate reservoirs. Section 2 defines the theoretical approach and methods used during the course of this study. Section 3 discusses wettability alteration as a means to reduce condensate blockage. Section 4

deals with the application of horizontal wells in gas condensate reservoirs. Section 5 includes discussion on Non Darcy flow effects and its impact on total gas production. Section 6 presents conclusions of this paper and proposes possible avenues for future work.

2. THEORETICAL APPROACH

2.1. Problem Statement

Among the many problems associated with gas condensate production, this thesis proposes three solutions to increasing well productivity in the North Field:

1. Wettability alteration
2. Horizontal wells
3. Reduction of Non Darcy flow

Wettability alteration to intermediate gas-wetting can enhance well deliverability in gas condensate reservoirs that experience a sharp drop in deliverability due to condensate dropout around the wellbore. Horizontal wells can improve productivity by minimizing pressure drop around the wellbore. The effect of Non Darcy flow is significant in a gas well, because Non Darcy flow decreases the production rate. A reduction in Non Darcy flow will therefore improve well performance. These problems will be discussed in this thesis.

2.1.1. General Methodology

The study is carried out with numerical reservoir simulation of fluid flow in a gas/gas condensate reservoir. A commercial simulator is adopted (Eclipse 3D compositional simulator, E300) and used in this thesis to study how well productivity can be enhanced in the North Field.

2.1.2. Wettability Alteration Study

Li and Firoozabadi (June 2000) developed a relative permeability model for gas condensate systems from a renormalization technique. They found that wettability alteration to intermediate gas wetting reduces critical condensate saturation

independently of gravity and interfacial tension. The model results of Li and Firoozabadi (June 2000) imply that wettability alteration near the wellbore may be the most effective method for increasing gas well deliverability. In 2000, Li and Firoozabadi became the first scientists to alter wettability through fluorochemical treatment. Li and Firoozabadi (April 2000) studied the effects of wettability alteration on liquid imbibition, oil drainage, permeability, and relative permeability in various porous media. They found that the wettability of gas-oil-rock systems can be altered from strong oil-wetting to preferential gas-wetting by FC-722, and that FC-722 is thermally stable and seems to alter wettability permanently. Tang and Firoozabadi (2000) studied the mobility of the gas and liquid phase before and after wettability alteration from strong liquid-wetting to intermediate gas-wetting. They established that the wettability of porous rocks can be altered to intermediate gas-wetting in gas-oil systems, which thereby significantly increases the liquid phase mobility. Fahes and Firoozabadi (2005) tested wettability alteration effects by measuring permeability, contact angle, imbibition, and flow testing in single and parallel cores. They found that wettability alteration from liquid-wetting to intermediate gas-wetting by chemical treatment at 140 degrees Celsius is permanent. Kumar *et al*. (2006) studied steady state gas-condensate relative permeability data before and after treatment with several fluorinated polymeric surfactants in methanol-water mixtures. They found that the productivity index improved 2 to 3 times for sandstone cores that had a temperature range of 145 to 275 degrees Fahrenheit and were treated with the Novec FC-4430 polymeric surfactant in the methanol-water mixture. This indicates that wettability alteration treatments can increase production at a low cost

since only the condensate blockage in the near wellbore region needs to be treated. Al-Anazi *et al*. (2007) evaluated the effectiveness of various chemical treatments in altering wettability of gas-condensate reservoirs from liquid wetting to intermediate gas wetting. They found that the effectiveness of the fluorochemical surfactant was affected by the treatment volume, aging time, core permeability, and temperature. Panga *et al*. (2007) presented a preventive and permanent chemical treatment for water removal and condensate blockage. They found that chemicals A5 and A6 were stable at high temperature and did not damage the cores, and that chemical A5 showed good wettability alteration along the cores. Wu and Firoozabadi (2009) studied the synergetic effect of salinity and fluorochemicals on the alteration of wettability from water-wetting to intermediate gas-wetting. They found that NaCl salinity increases water-wetting when a core is saturated with brine. This study will use a 3D reservoir simulator to test if wettability alteration can successfully be used in the North Field to increase gas well deliverability. An oil-wet reservoir will be simulated with one set of relative permeability data, and an intermediate-wet reservoir will be simulated with another set of relative permeability. Both simulations will have the exact same reservoir and fluid properties, and both wells will be produced for the same length of time.

2.1.3. Horizontal Well Application in Gas/Gas Condensate Reservoirs

Muladi and Pinczewski (1999) examined the difference in production performance between horizontal and vertical wells for different heterogeneities in a gas condensate reservoir. They found that horizontal wells have better performance than vertical wells when horizontal wells are applied in high average permeability reservoirs.

Dehane *et al*. (2000) investigated the performance of horizontal wells and vertical wells in gas condensate reservoirs under various depletion schemes. They found that horizontal wells have a smaller drawdown pressure than vertical wells in a gas condensate reservoir, and they conclude that the liquid deposit can be reduced by using horizontal wells. For wells produced at the same rate and time period, Dehane *et al*. (2000) found that liquid saturation near a vertical well can reach 15% while liquid saturation around a horizontal well does not exceed 6%. Harisch et al. (2001) evaluated a horizontal gas condensate well using numerical pressure transient analysis techniques. They found that multiphase effects had little impact on the pressure response of the system while horizontal well fluid flow regimes appeared to be the controlling factor. Hashemi and Gringarten (2005) used reservoir simulation to quantify the increase in well productivity from different remediation solutions. They found that horizontal wells not only increase productivity in dry gas systems, but they also perform better in gas condensate reservoirs below the dew point since they decrease pressure drawdown and condensate blockage. We will use a 3D reservoir simulator to test if horizontal wells can increase productivity more effectively than vertical wells, specifically, in the Khuff formation located in the North Field. Drawdown pressures for a North Field horizontal well will be compared with the drawdown pressures of a North Field vertical well, then a horizontal well productivity index will be compared with a vertical well productivity index.

2.1.4. Method for Reduction of Non Darcy Flow Study

A 3D reservoir simulator is used to study Non Darcy flow in both a multilateral well and a vertical well. A Non Darcy flow sensitivity test is run to see the impact Non Darcy flow has on near wellbore condensate blockage, and therefore, gas well productivity.

2.2. PVT Analysis

To simulate the defined problem, an equation of state is required to describe the fluid behavior at certain temperatures and pressures. A composition PVT equation of state based program is used to characterize a set of fluid samples obtained from Whitson and Kuntadi (2005). A compositional PVT program allows reservoir fluid samples to have a realistic physical model in a reservoir simulation. Differences between the measured and calculated data are minimized using a regression facility which adjusts various equation of state parameters. The equation of state for a real fluid is:

$$PV = nRTZ \tag{2.1}$$

P is the pressure, V is the volume, n is the number of moles, R is the universal gas constant, T is the temperature, and Z is the compressibility factor obtained from the solution of Eq. (2.4). The Soave-Redlich-Kwong equation of state is implemented in the simulation via Martin's generalized equation. Martin (1979) showed that all forms of cubic equations can be obtained from the following equation:

$$P = \frac{RT}{V} - \frac{\alpha(T)}{(V+\beta)(V+\gamma)} + \frac{\delta(T)}{V(V+\beta)(V+\gamma)} \tag{2.2}$$

R is the universal gas constant, α and δ are functions of temperature,

and β and γ are constants. Coats (1982) took Eq. (2.2) and used basic thermodynamic relationships to get the following equation:

$$z^3+[(m_1+m_2-1)B-1]z^2+[A+m_1m_2B^2-(m_1+m_2)B(B+1)]z \\ -[AB+m_1m_2B^2(B+1)]=0 \tag{2.3}$$

which can be rearranged to form the following equations:

$$Z^3+E_2Z^2+E_1Z+E_0=0 \tag{2.4}$$

where:

$$E_2=(m_1+m_2-1)B-1 \tag{2.5}$$

$$E_1=A-(m_1+m_2-m_1m_2)B^2-(m_1+m_2)B \tag{2.6}$$

$$E_0=-[AB+m_1m_2B^2(B+1)] \tag{2.7}$$

Coefficient m_1 = 0 and coefficient m_2 =1. The cubic equation for the Z-factor can be solved to obtain Z-factors for the liquid and vapor phases. Since Eq. (2.4) is a cubic function, three solutions are usually obtained. The smallest Z-factor is chosen for the liquid phase, and the largest Z-factor is chosen for the vapor phase. The Fugacity coefficients are found using the equation:

(2.8)

$$\ln(f_i/(px_i))=-\ln(Z-B)+\frac{A}{(m_1-m_2)B}\left(\frac{2\sum_i}{A}-\frac{B_i}{B}\right)\ln\left(\frac{Z+m_2B}{Z+m_1B}\right)+\frac{B_i}{B}(Z-1)$$

The following four equations are used in Eq. (2.8), and are the mixing laws used in all equations of state:

$$\sum_i=\sum_j A_{ij}x_j \tag{2.9}$$

$$A = \sum_{j=1}^{n}\sum_{k=1}^{n} x_j x_k A_{jk} \tag{2.10}$$

$$B = \sum_{j=1}^{n} x_j B_j \tag{2.11}$$

$$A_{jk} = (1-\delta_{jk})(A_j A_k)^{1/2} \tag{2.12}$$

The variables in Eqs. (2.9-2.12) are defined by:

$$A_j = \Omega_a(T, j)\frac{P_{rj}}{T_{rj}^2} \tag{2.13}$$

$$B_j = \Omega_b(T, j)\frac{P_{rj}}{T_{rj}} \tag{2.14}$$

δ_{jk} are binary interaction coefficients between hydrocarbons and non-hydrocarbons, and $\Omega_a(T, j)$ and $\Omega_b(T, j)$ are functions of the acentric factor, w_j , and the reduced temperature, T_{rj} . For the Soave-Redlich-Kwong equation of state, the equations are:

$$\Omega_b = (T, j) = \Omega_{a_o}[1+(0.48+1.574w_j - 0.176w_j^2)(1-T_{rj}^{1/2})]^2 \tag{2.15}$$

$$\Omega_b(T, j) = \Omega_{b_o} \tag{2.16}$$

Ω_{a_o} and Ω_{b_o} are constants in the above equations with values of Ω_{a_o} = 0.4274802 and Ω_{b_o} = 0.08664035. The surface tension between the liquid and vapor phase of a multi-component mixture can be estimated using the Macleod-Sugden equation:

$$\sigma_{mix}^{1/4} = \sum_{i=1}^{N_c}[P_i](\rho_m^{Liq}x_i - \rho_m^{Vap}y_i) \tag{2.17}$$

$[P_i]$ is the parachor of the i^{th} component which has a liquid and vapor mole fraction of x_i and y_i respectively, and the liquid and vapor molar densities are ρ_m^{Liq} and ρ_m^{Vap} respectively. The equation of state model is then tuned by regression. Once the

model has been tuned, it is exported into the simulator. The flash is used to simulate the experiments and predict values for experimental observations. Once the Soave-Redlich-Kwong equation of state is chosen, the fugacities can be directly calculated. The liquid and vapor phases must be equal for each component in a thermodynamic system to be in equilibrium:

$$f_{iL} = f_{iV} \tag{2.18}$$

Lohrenz *et al*. (1964) developed procedures to calculate the viscosities of in situ reservoir gases and liquids from composition. Their method, the Lohrenz-Bray-Clark method, is used to find the viscosity values in compositional simulation. The viscosity μ for each phase is:

$$[(\mu - \mu^o) \cdot \delta + 0.0001]^{1/4} = \sum_{i=1} a_i \cdot b_r^{i-1} \tag{2.19}$$

μ^o and δ are functions of the composition, component molecular weights, critical pressures, and critical temperatures. The coefficients a_i are 0.1023, 0.023364, 0.058533, -0.040758, and 0.0093324 which are default values found by Lohrenz *et al.* (1964). The equation for reduced molar density is:

$$b_r = \frac{b_p}{b_c} \tag{2.20}$$

The phase volumes, b_p, are found from the pressure and compressibility. For each phase, the critical molar density, b_c, is:

$$\frac{1}{b_c} = V_c = \sum x_i \cdot V_{c,i} \tag{2.21}$$

Constant Volume Depletion (CVD) experiments are useful in modeling gas condensate

reservoirs. In a gas condensate reservoir, gas and oil do not move much with respect to each other because liquid does not reach a high enough saturation to become mobile as the pressure drops. This is why CVD experiments model gas condensate reservoirs extremely well.

2.3. Reservoir Description

2.3.1. Geological Model

The geological properties used to create the reservoir simulation models for this thesis are based on data from Whitson and Kuntadi (2005). The Khuff formation is made up of fine-to-coarse crystalline dolomite with some interbeds of limestone and anhydrite (Khalaf 1997). There are four non-communicating Khuff geological layers: K1 which is about 204 ft thick, K2 which is 327 ft thick, K3 which is 255 ft thick, and K4 which is 645 ft thick. The non-communicating layer between K1 and K2 is made of 3.28 ft of anhydrite. The non-communicating 3.28 ft thick layer that separates K2 and K3 consists of mudstone and anhydrite. The non-communicating layer that separates K3 and K4 consists of 142.86 ft of anhydrite (Whitson and Kuntadi 2005). High-permeability along with low-thickness layers consisting of vugs and fractures are the major geological features that characterize the Khuff formation. The Khuff formation is the main geologic unit that makes up Qatar's North Field. Fig. 4 shows a map of the North Field.

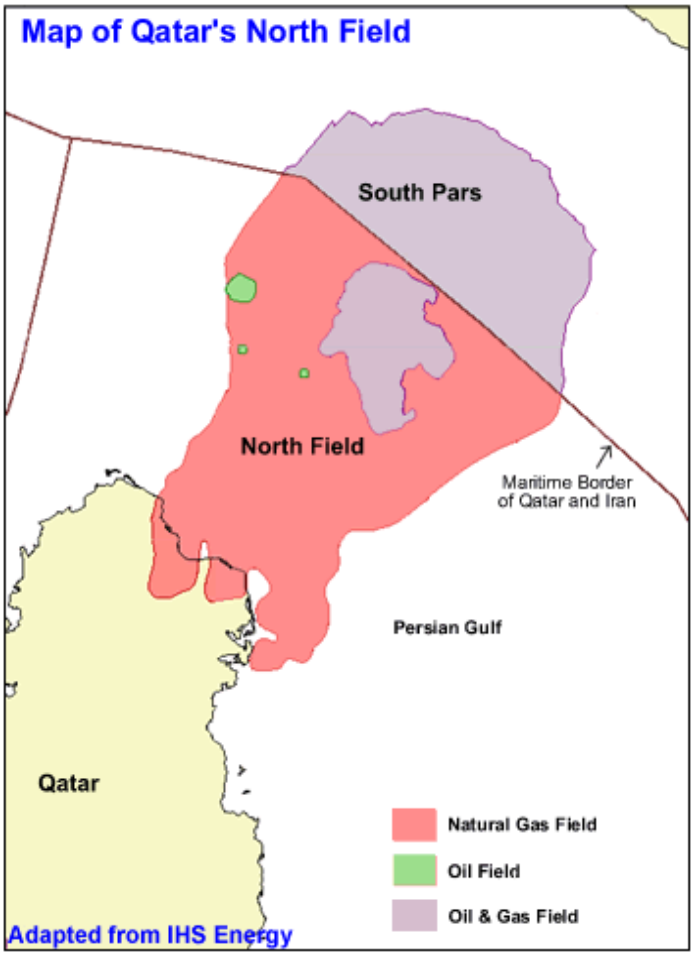

Fig. 4: Map of North Field

Table 1 shows the rock properties obtained from Whitson and Kuntadi (2005).

K1 and K4 have a constant porosity of 0.10 while K2 and K3 have a constant porosity of 0.15. The top of the formation starts 8,050 ft below the ground surface.

Table 1: Rock Properties

Rock Properties	
K1 Porosity	0.10
K2 Porosity	0.15
K3 Porosity	0.15
K4 Porosity	0.10
Rock Compressibility (1/psi)	5.00E-06
Reservoir Temperature (F)	220.0
Depth to Top of Formation (ft)	8,050

Fig. 5 shows the unique horizontal permeability distribution of the North Field. Each geologic unit (K1, K2, K3, and K4) has a 10 ft thick, high permeability layer in the center of the layer. This high permeability layer is indicated by the thick black lines in Fig. 5. Low permeability regions extend above and below the 10 ft high permeability layer for each geologic unit. The permeability in the x-direction is equal to the permeability in the y-direction, while the permeability in the vertical direction is 1/10 the permeability in the horizontal directions.

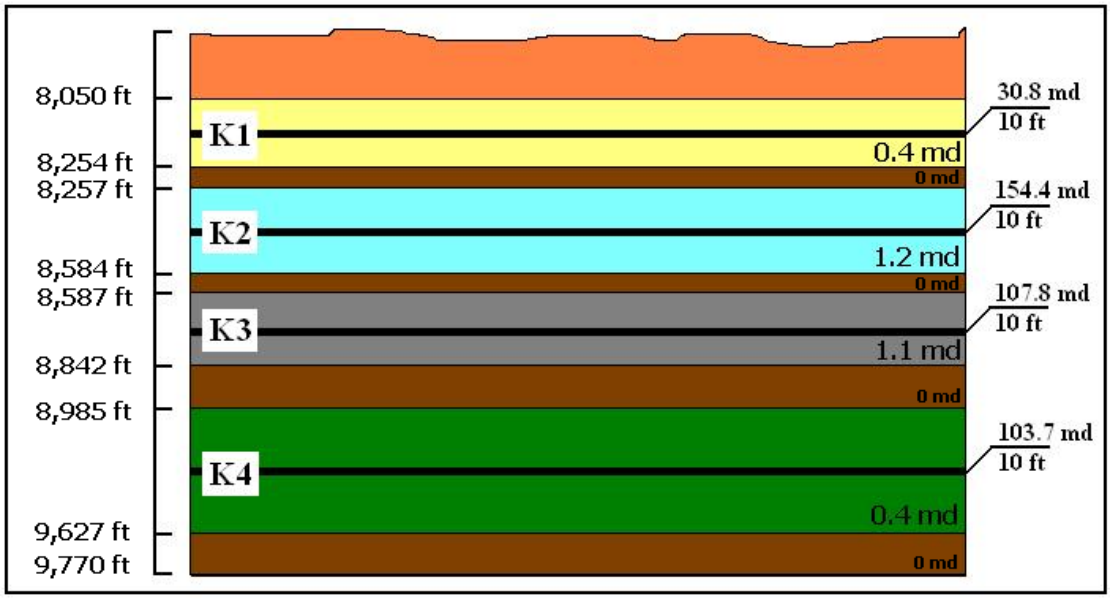

Fig. 5: Horizontal Reservoir Permeability

Table 2 shows that K1 and K4 share an identical initial pressure value of 5,315 psia and a dew point pressure value of 5,135 psia. K2 and K3 have a similar initial pressure value of 5,205 psia and a dew point pressure value of 4,945 psia.

Table 2: Initial Conditions

Initial Conditions	
K1 Initial Pressure (psia)	5,315
K2 Initial Pressure (psia)	5,205
K3 Initial Pressure (psia)	5,205
K4 Initial Pressure (psia)	5,315
K1 Dew Point Pressure (psia)	5,135
K2 Dew Point Pressure (psia)	4,945
K3 Dew Point Pressure (psia)	4,945
K4 Dew Point Pressure (psia)	5,135

Table 3 shows the relative permeability endpoints used by Whitson and Kuntadi (2005) in order to develop relative permeability curves that accurately model the North Field.

Table 3: Relative Permeability

Relative Permeability	
Connate Water Saturation (Swc)	0.20
Residual Oil Saturation to Water (Sorw)	0.20
Residual Oil Saturation to Gas (Sorg)	0.20
Critical Gas Saturation (Sgc)	0.10
Water Relative Permeability at Sw=1-Sorw, Sg=0 (krwro)	0.50
Gas Relative Permeability at Sw=Swc, So=Sorg (krgro)	0.33
Oil Relative Permeability at Sw=Swc, So=0 (krocw)	0.90

Table 4 shows the equation of state parameters that are used in order to model the North Field (Whitson and Kuntadi 2005). The acentric factors, w_j, in column five of Table 4 are variables that are directly input into Eq. (2.15) to further define the mixing laws. The volume shifts, $\sum_i$, in column seven of Table 4 are input into Eq. (2.8) to determine the Fugacity coefficients. The parachors, $[P_i]$, in column six of Table 4 are input into Eq. (2.17) to determine the surface tension between the liquid and vapor phase of a multi-component mixture.

Table 4: Equation of State Parameters

Component	MW	Pc (psia)	Tc (R)	Acentric Factors	Parachors	Volume Shifts	Zc
N2	28.014	492.84	227.16	0.037	59.1	-0.0009	0.29178
H2S	34.082	1299.97	672.12	0.09	80.1	0.1015	0.28292
CO2	44.01	1069.51	547.42	0.225	80	0.2175	0.27433
C1	16.043	667.03	343.01	0.011	71	-0.0025	0.2862
C2	30.07	706.62	549.58	0.099	111	0.0589	0.27924
C3	44.097	616.12	665.69	0.152	151	0.0908	0.2763
i-C4	58.123	527.94	734.13	0.186	188.8	0.1095	0.28199
n-C4	58.123	550.56	765.22	0.2	191	0.1103	0.27385
i-C5	72.15	490.37	828.7	0.229	227.4	0.0977	0.27231
n-C5	72.15	488.78	845.46	0.252	231	0.1195	0.26837
C6	82.319	491.32	924.21	0.23726	232.57	0.1341	0.27034
C7	95.357	457.18	988.34	0.27142	263.86	0.1429	0.26589
C8	108.772	422.82	1043.92	0.30936	296.05	0.1522	0.2614
C9	121.895	389.97	1094.09	0.35002	327.55	0.1697	0.25713
C10	134.784	361.66	1138.55	0.38996	358.48	0.1862	0.25334
C11	147.589	336.96	1178.85	0.42946	389.21	0.2018	0.24986
C12	160.302	315.31	1215.63	0.4684	419.72	0.2165	0.2466
C13	172.914	296.27	1249.41	0.50673	449.99	0.2302	0.24352
C14	185.422	279.43	1280.57	0.54442	480.01	0.243	0.24056
C15	197.823	264.48	1309.45	0.58144	509.77	0.2548	0.2377
C16	210.113	251.14	1336.33	0.6178	539.27	0.2657	0.23493
C17-19	233.389	229.29	1383.11	0.68566	595.13	0.2843	0.22981
C20-29	299.514	184.61	1493.68	0.87122	753.83	0.3239	0.2161
C30+	477.341	167.56	1616.94	1.04107	1180.62	0.1154	0.20582

Table 5 shows the Binary Interaction Coefficients that were used in order to accurately imitate the results of Whitson and Kuntadi (2005). The binary interaction coefficients are used in Eq. (2.12).

Table 5: Binary Interaction Coefficients

Component	N2	CO2	H2S
N2	0	0	0.12
CO2	0	0	0.12
H2S	0.12	0.12	0
C1	0.02	0.12	0.07
C2	0.06	0.15	0.06
C3	0.08	0.15	0.06
iC4	0.08	0.15	0.06
nC4	0.08	0.15	0.06
iC5	0.08	0.15	0.06
nC5	0.08	0.15	0.06
C6	0.08	0.15	0.05
C7	0.08	0.15	0.03
C8	0.08	0.15	0.03
C9	0.08	0.15	0.03
C10	0.08	0.15	0.03
C11	0.08	0.15	0.03
C12	0.08	0.15	0.03
C13	0.08	0.15	0.03
C14	0.08	0.15	0.03
C15	0.08	0.15	0.03
C16	0.08	0.15	0.03
C17-19	0.08	0.15	0.03
C20-29	0.08	0.15	0.03

The data from Table 4 and Table 5 is used in the Soave-Redlich-Kwong version of Eq. (2.1) in order to characterize North Field fluids. Once the data in Fig. 5 and Table 1 through Table 6 were input into the simulator, the gas rate decline results were generated. The results from the simulation were compared with the EOS results presented in the original study by Whitson and Kuntadi (2005). Fig. 6 shows the match for the gas rate decline curve is satisfactory since the Whitson and Kuntadi (2005) gas production rate declines after 4,195 days, and the Eclipse EOS model declines after 4,174 days resulting in a 0.5% error. The reason that both gas production rate curves

decreased at a time period approaching 4,200 days is due to the fact that a minimum bottom hole pressure of 2,500 psi is reached. The simulator is programmed so that the control data for the producing well switches from a constant gas rate target to a bottom hole pressure target when a bottom hole pressure of 2,500 psia has been approached.

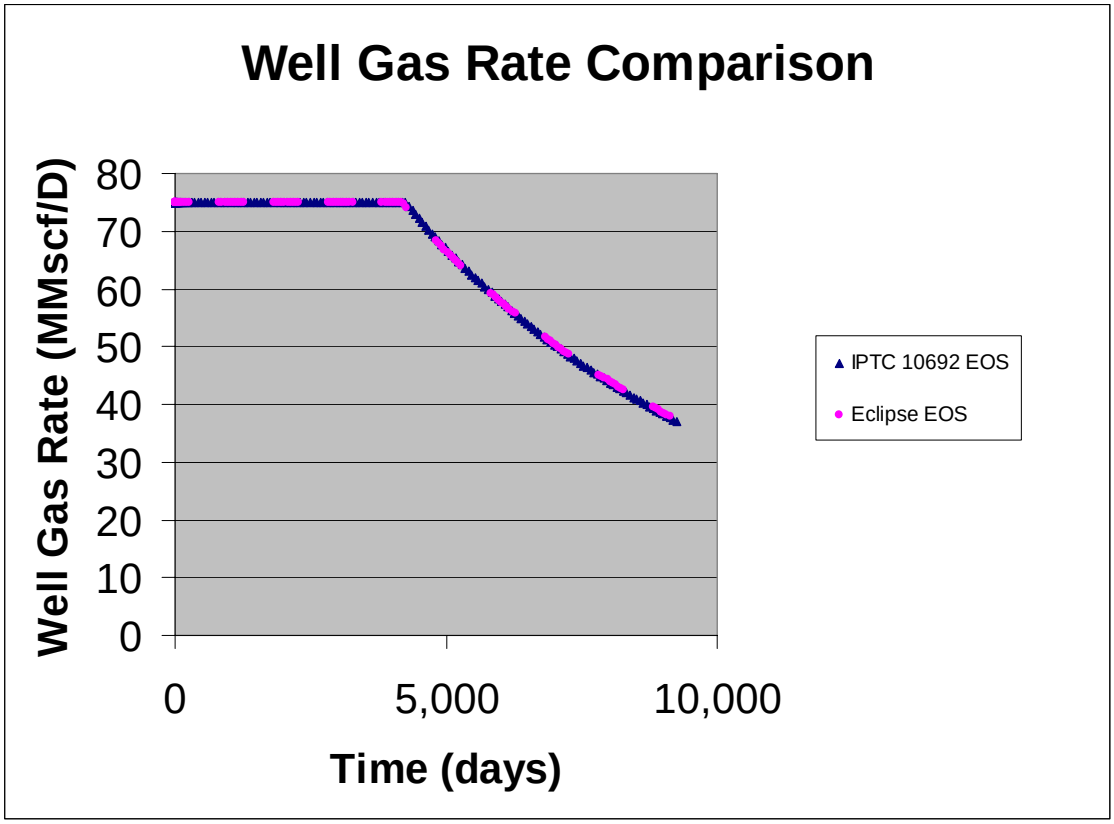

Fig. 6: Well Gas Rate Production Match with IPTC 10692

2.3.2. Fluid Properties

Khuff formation reservoir fluids typically have a condensate gas ratio ranging from 30 to 100 stb/MMscf and a methane content ranging from 65 to 85 percent moles.

C6+ ranges from 1.5 to 4.5 percent moles, and non-hydrocarbon content includes small amounts of N2 and CO2 (Whitson and Kuntadi 2005). Table 6 shows the fluid composition obtained for all four hydrocarbon layers: K1, K2, K3, and K4. Table 6 shows that K1 and K4 are similar in composition, and K2 and K3 are similar in composition.

Table 6: Fluid Composition

Component	K1 (% moles)	K2 (% moles)	K3 (% moles)	K4 (% moles)
N2	3.349	3.349	3.349	3.349
H2S	0.529	3.029	3.029	0.529
CO2	1.755	1.755	1.755	1.755
C1	83.265	80.765	80.765	83.265
C2	5.158	5.158	5.158	5.158
C3	1.907	1.907	1.907	1.907
iC4	0.409	0.409	0.409	0.409
nC4	0.699	0.699	0.699	0.699
iC5	0.280	0.280	0.280	0.280
nC5	0.280	0.280	0.280	0.280
C6	0.390	0.390	0.390	0.390
C7	0.486	0.486	0.486	0.486
C8	0.361	0.361	0.361	0.361
C9	0.266	0.266	0.266	0.266
C10	0.201	0.201	0.201	0.201
C11	0.153	0.153	0.153	0.153
C12	0.116	0.116	0.116	0.116
C13	0.089	0.089	0.089	0.089
C14	0.068	0.068	0.068	0.068
C15	0.052	0.052	0.052	0.052
C16	0.040	0.040	0.040	0.040
C17-19	0.073	0.073	0.073	0.073
C20-29	0.063	0.063	0.063	0.063
C30+	0.011	0.011	0.011	0.011

Table 7 shows the fluid properties used to describe the North Field fluid (Whitson and Kuntadi 2005).

Table 7: Fluid Properties

Fluid Properties	
Water Compressibility (1/psi)	2.64E-06
Water FVF (rb/stb)	1.0375
Water Density (lbs/cuft)	62.37
Water Viscosity (cp)	0.65

2.4. Well Models

Three well models were developed: a vertical well model, a multilateral well model, and a horizontal well model (derived from the multilateral well model). The vertical well model was modeled in radial coordinates, while the multilateral well was modeled with Cartesian coordinates.

2.4.1. Vertical Wellbore

Fig. 7 shows that the vertical well is 1.116 ft in diameter, and extends 1,720.24 ft in height. The low permeability regions are indicated in yellow, the high permeability regions are indicated in blue, and the non-communicating layers are indicated in brown.

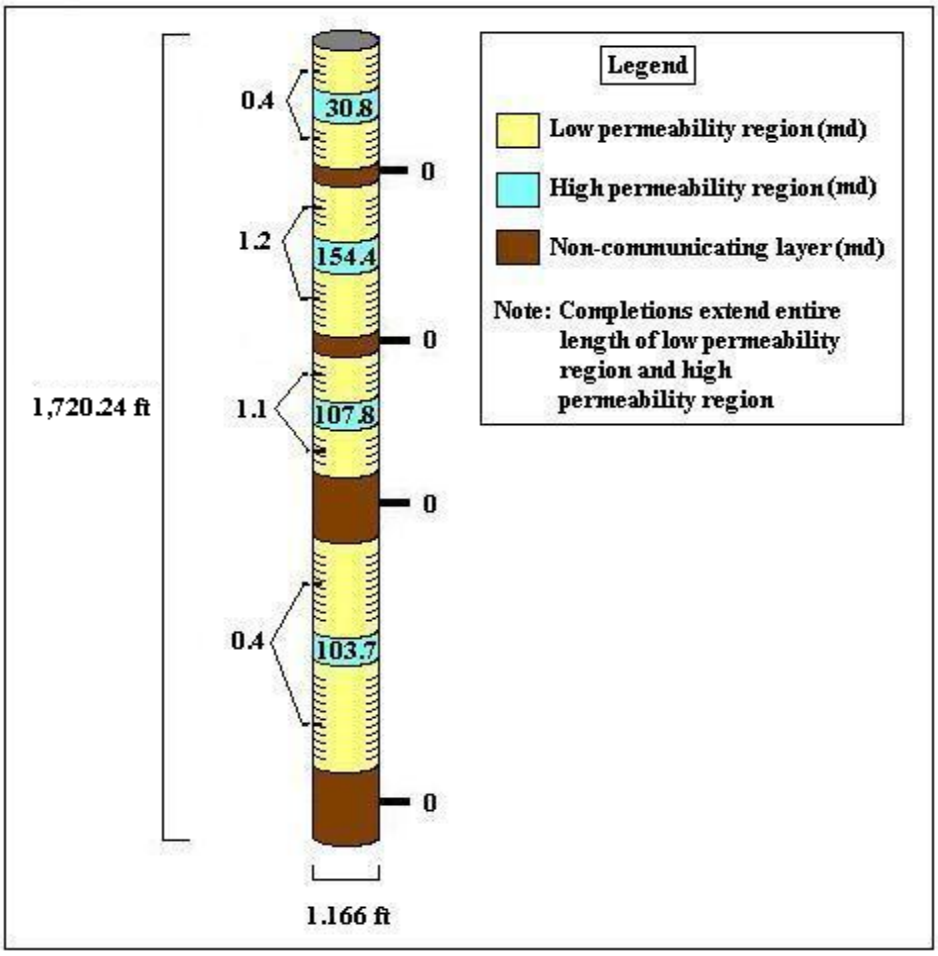

Fig. 7: Vertical Well Model

Fig. 8 shows the vertical well reservoir model. Radial coordinates are used to define the 3,625 grid blocks. The large green ring (middle of reservoir model) and the large red ring (bottom of reservoir model) are non communicating layers that extend 142.86 ft each in the vertical direction.

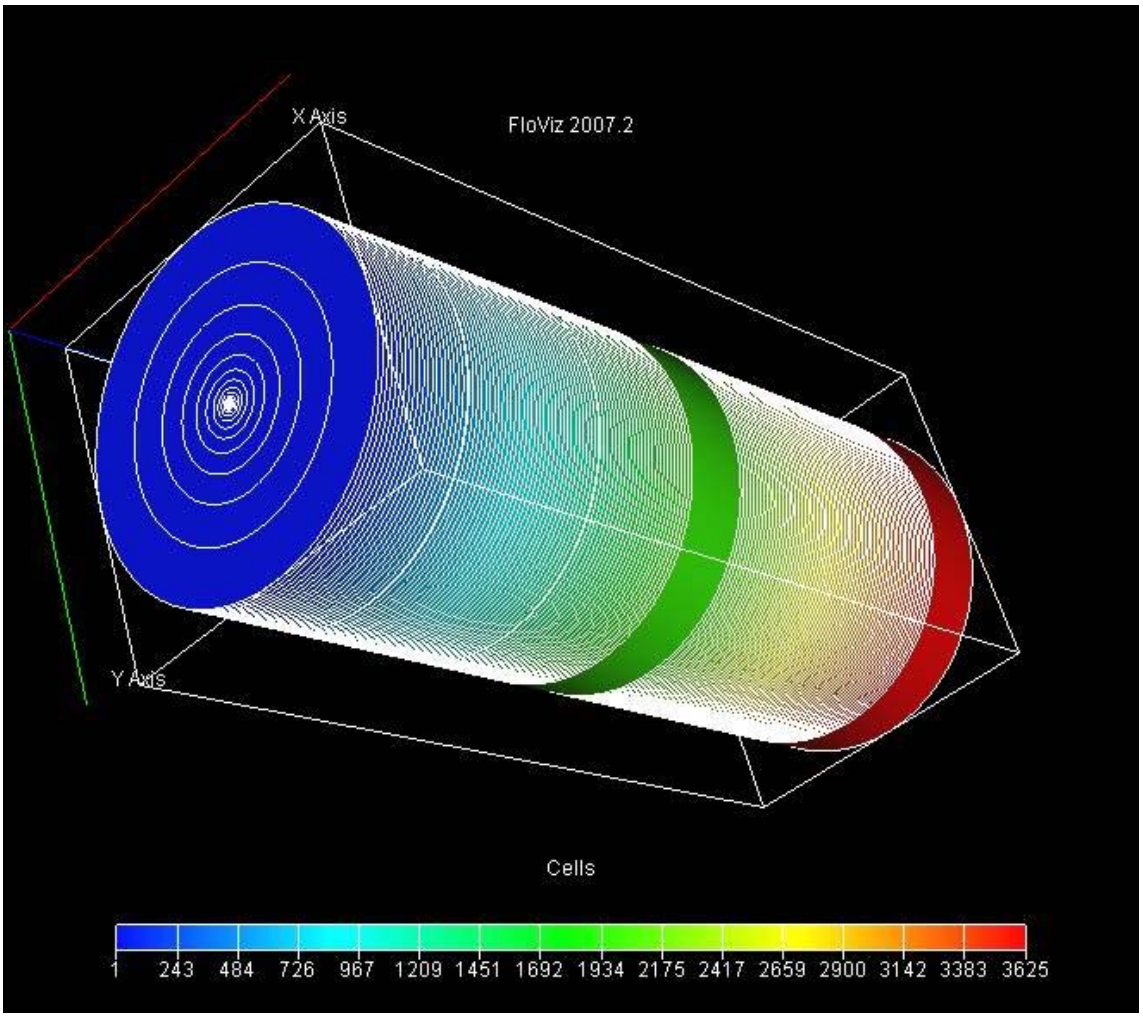

Fig. 8: Reservoir Model for Vertical Well

Table 8 shows the base grid block model used for all vertical well simulations in this thesis. The well radius, r_w, is .528 ft and is followed by 25 grid blocks with each block thickness given in column two of Table 8.

Table 8: Radial Grid Block Increments

R-Coordinate Grid	Radius Increment (ft)
r_w	0.528
1	0.25
2	0.35
3	0.5
4	0.72
5	1.03
6	1.46
7	2.09
8	2.97
9	4.24
10	6.04
11	8.62
12	12.29
13	17.52
14	24.98
15	35.61
16	50.78
17	72.4
18	103.22
19	147.17
20	209.83
21	299.17
22	426.56
23	608.17
24	867.13
25	1236.33

Table 9 shows the grid block thickness for the vertical direction in the vertical well model. There are 145 grid blocks in the vertical direction and each of the 145 grid blocks varies in thickness as shown in Table 9.

Table 9: Vertical Grid Block Increments

Z-Coordinate Grid	Individual Grid Block Thickness (ft)
Block 1 through Block 20	10.2
Block 21	3.28
Block 22 Through Block 53	10.2
Block 54	3.28
Block 55 through Block 79	10.2
Block 80	142.86
Block 81 through Block 144	10.04
Block 145	142.86

2.4.2. Multilateral Wellbore

Fig. 9 shows the multilateral wellbore model. Each lateral has a diameter of 0.583 ft and a length of 945 ft. Low permeability regions are shown in yellow, high permeability regions are shown in blue, and non-communicating layers are shown in brown.

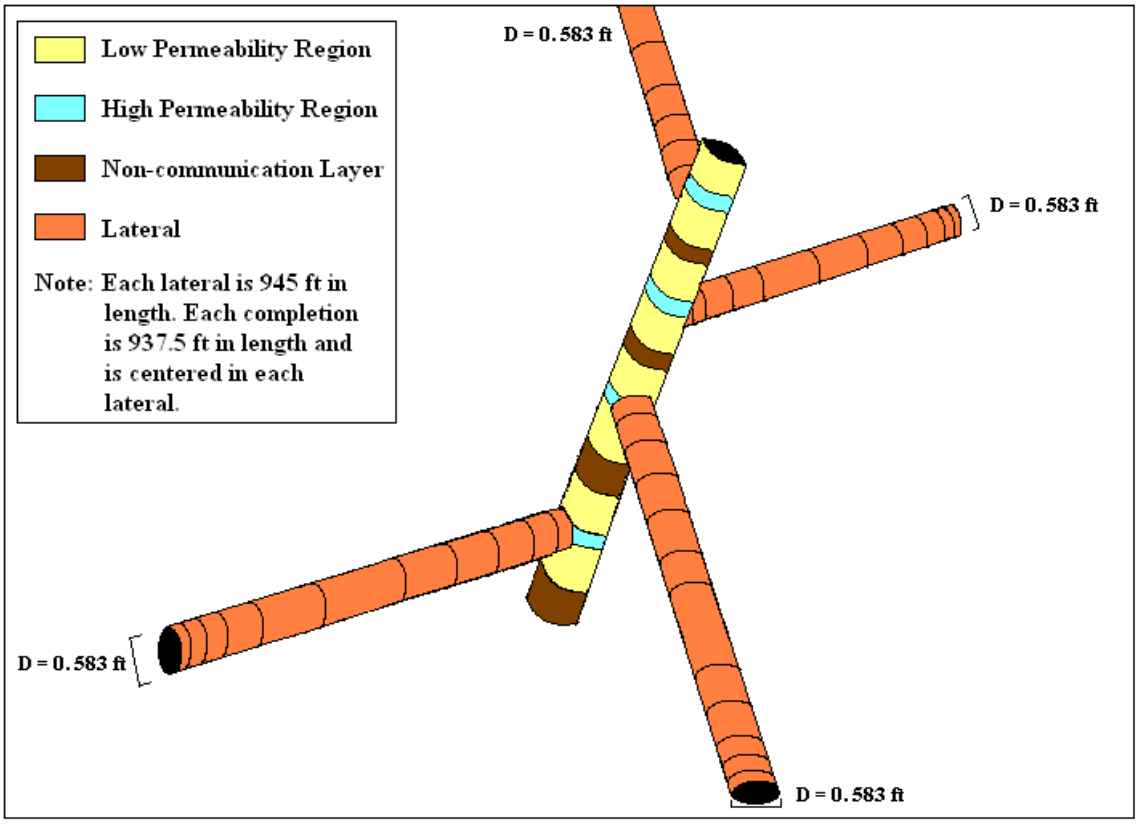

Fig. 9: Multilateral Well Model

Fig. 10 shows the multilateral well reservoir model. The vertical wellbore of the multilateral well is located in the center of the reservoir, and the total number of grid blocks used in the multilateral well reservoir model is 13,456.

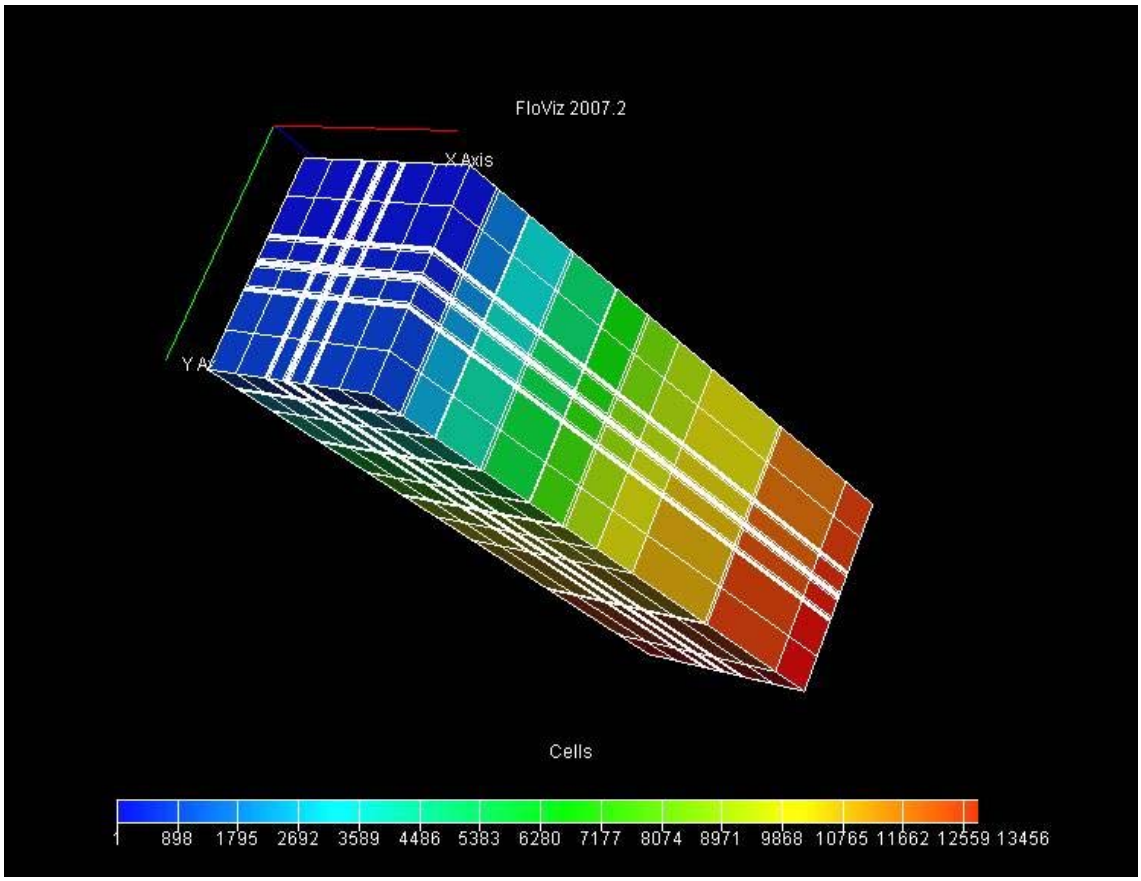

Fig. 10: Reservoir Model for Multilateral Well

Table 10 shows the base grid block model used for all multilateral well simulations in this thesis. There are 29 grid blocks in the x-direction, 29 grid blocks in the y-direction, and 16 grid blocks in the z-direction. Large grid block sizes of 1345.75 ft had to be used at the edges of the reservoir in order to:

1. Match the reservoir volumes used in previous work (Whitson and Kuntadi 2005)
2. Stay within the limitations placed on the total number of grid blocks used in a simulation (Texas A&M Eclipse simulation license)

Table 10: Grid Block Model for Multilateral Well (29x29x16)

X-Coordinate Grid	Block Thickness (ft)	Y-Coordinate Grid	Block Thickness (ft)	Z-Coordinate Grid	Block Thickness (ft)
1	1345.74	1	1345.74	1	91.8
2	1345.74	2	1345.74	2	10.2
3	20	3	20	3	102
4	10	4	10	4	3.28
5	5	5	5	5	153
6	10	6	10	6	10.2
7	20	7	20	7	163.2
8	40	8	40	8	3.28
9	80	9	80	9	122.4
10	640	10	640	10	10.2
11	80	11	80	11	122.4
12	40	12	40	12	142.86
13	20	13	20	13	311.24
14	10	14	10	14	10.04
15	5	15	5	15	321.28
16	10	16	10	16	142.86
17	20	17	20		
18	40	18	40		
19	80	19	80		
20	640	20	640		
21	80	21	80		
22	40	22	40		
23	20	23	20		
24	10	24	10		
25	5	25	5		
26	10	26	10		
27	20	27	20		
28	1345.74	28	1345.74		
29	1345.74	29	1345.74		

2.5. Further Developments

Further work could be done by incorporating intelligent well valves and chokes into the horizontal and multilateral well models since DATA files have been created. Smaller grid block sizes (which lead to more accurate results) could be implemented if

the Texas A&M license could be upgraded to allow more simulation blocks to be used during simulation runs.

3. USING WETTABILITY ALTERATION TO REDUCE CONDENSATE BLOCKAGE IN THE NORTH FIELD

3.1. Overview

This section will explain how wettability alteration can be used to reduce condensate blockage, thereby increasing total gas production. Li and Firoozabadi (April 2000) have shown that a permanent intermediate gas wetting can be established in Berea core samples through chemical treatment. Based on this observation, and relative permeability data taken from Tang and Firoozabadi (2000), this section explores a field application of wettability alteration in the North Field.

3.2. Wettability Definition

Wettability is the tendency of a solid to be in contact with a specific phase over another phase (Schlumberger, 2009). For instance liquid-wet is the tendency of a solid to be in contact with a liquid phase rather than a gas phase. Gas-wet is the tendency of a solid to be in contact with a gas phase rather than a liquid phase. Intermediate-wet is a wettability case between liquid-wet and gas-wet.

3.3. The Statement of the Problem

When the reservoir pressure in the near wellbore region decreases below the dew point pressure, a condensate ring forms around the wellbore. The condensate saturation in this region will be higher than predicted by PVT laboratory work because of relative permeability effects. El-Banbi *et al*. (2000) found that production rates decline in gas condensate wells (in low permeability reservoirs) because of liquid drop out around the wellbore. They validated this conclusion via Fig. 11, which shows that the gas

production rate drops rapidly during the first 5 years of production. After the dew point pressure is reached, condensate builds up which causes gas moving to the wellbore to become leaner, and liquid to become heavier. At this point, the mobility of gas is increased due to increased liquid viscosity and decreased gas viscosity (El-Banbi *et al*. 2000).

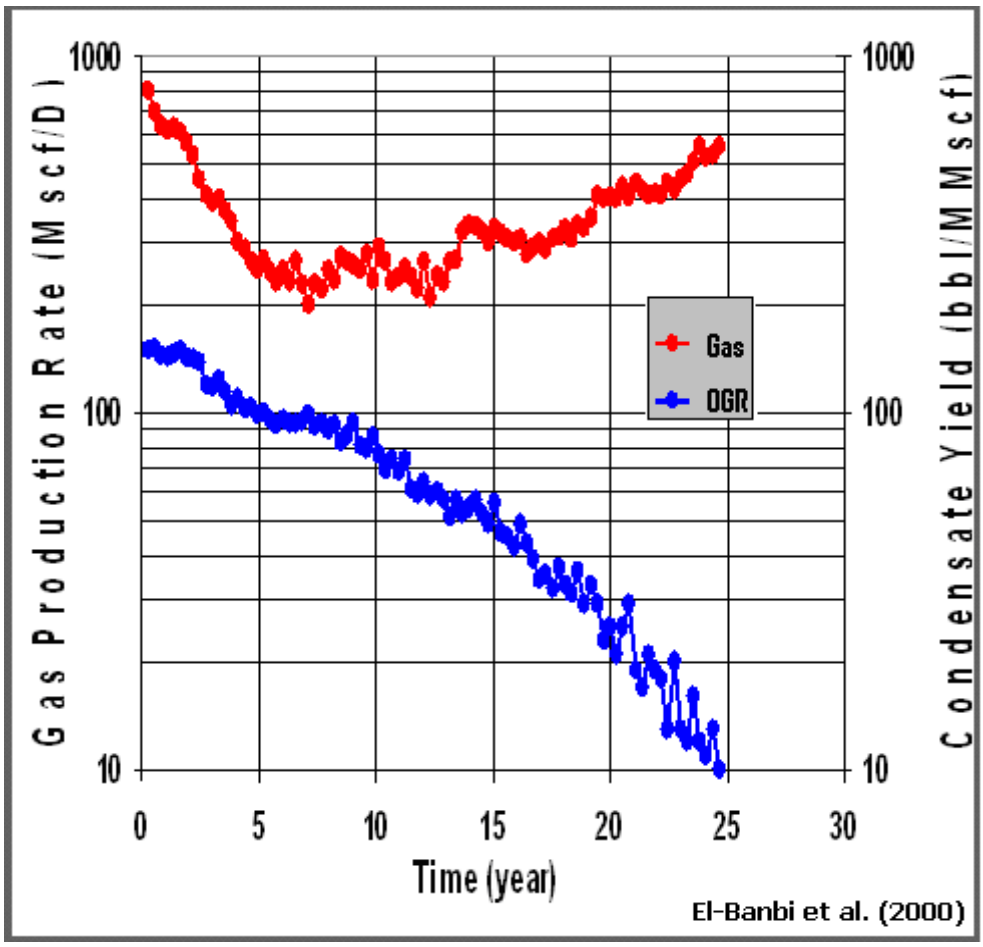

Fig. 11: Condensate Blockage

Fig. 12 shows an example of what happens when the pressure in a reservoir approaches the dew point pressure. Fig. 12 shows that when the block pressure drops below the dew point pressure of 5,135 psi, oil starts to form in each grid block. After this point, oil saturation continues to increase as reservoir pressure continually declines.

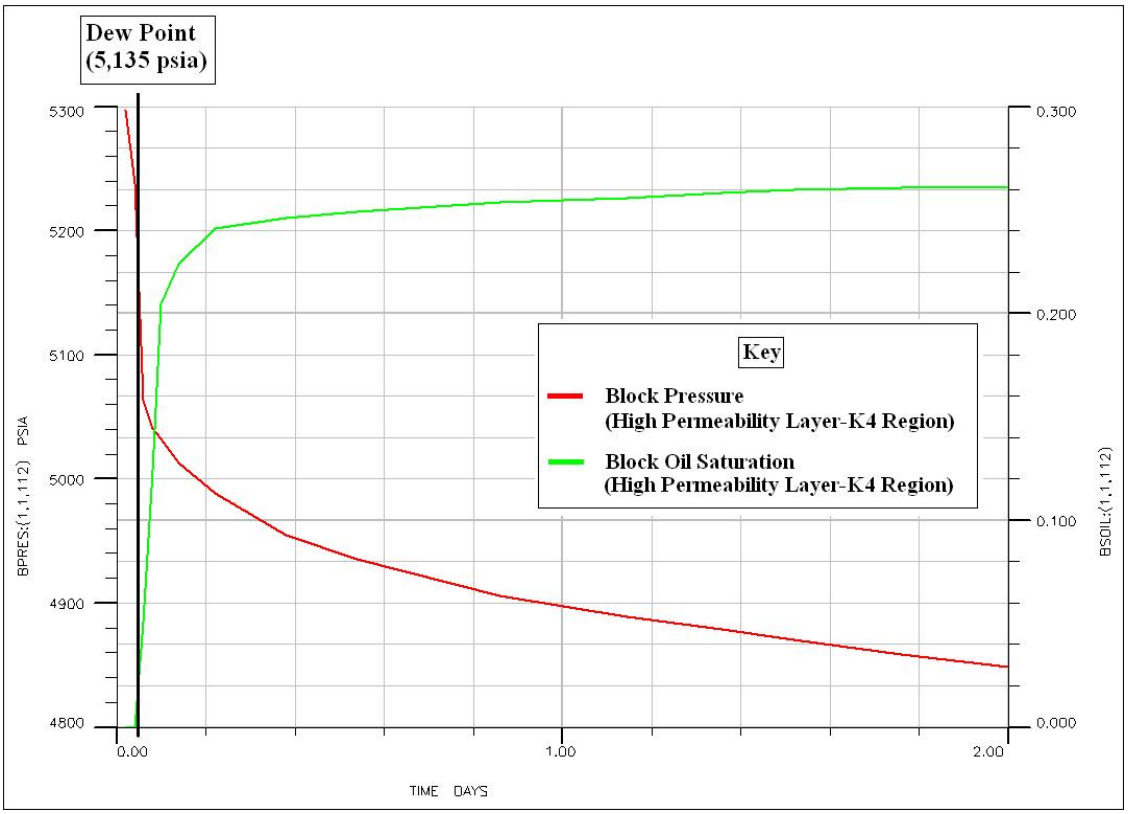

Fig. 12: Oil Saturation vs. Dew Point

3.4. Wettability Alteration

Wettability is an important factor in condensate accumulation around the wellbore, and it can be explained using the Young-Laplace equation (Tang and Firoozabadi 2000):

$$P_c = \frac{2\sigma\cos\theta}{r} \tag{3.1}$$

P_c is capillary pressure, σ is interfacial tension, θ is contact angle, and r is pore size. Condensate accumulation around the wellbore can be reduced if interfacial tension is decreased, or the contact angle is decreased. Previous work (Li and Firoozabadi June 2000) shows that the best way to reduce critical condensate saturation through wettability, is by decreasing the contact angle. The contact angle, or wetting angle, is a thermodynamic variable that depends on the interfacial tensions of the surfaces. In Fig. 13, if theta is between 0 and 90 degrees the surface is said to be gas-wet. If theta is between 90 and 180, the surface is said to be oil wet. If the contact angle is 180 degrees, the matrix is said to be perfectly wettable.

Fig. 13: Contact Angle Definition

Fig. 14 shows a further depiction of fluid wettability. The two images on the left describe an oil-wet surface and the two images on the right describe a gas-wet surface. The oil-wet surface shows that the oil is absorbing into the surface and is bound while the gas flows on through the rock. The gas-wet surface shows the gas absorbing into the

surface while the oil shows absorption resistance.

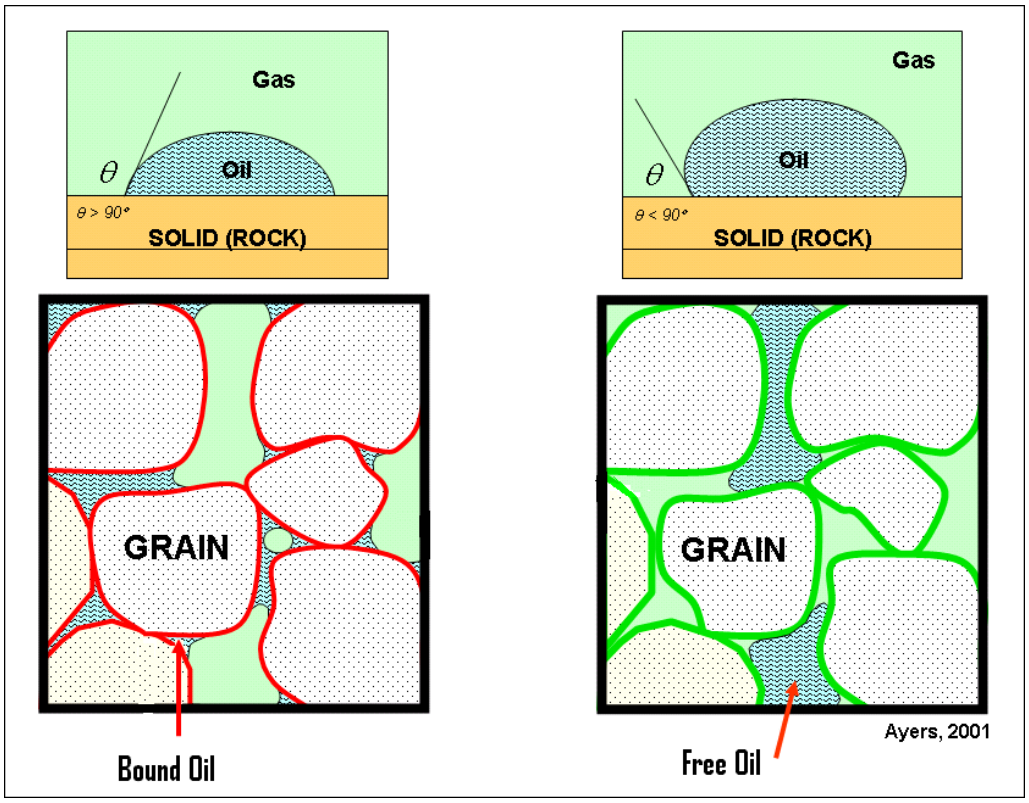

Fig. 14: Contact Angle and Pore View

The idea of wettability alteration is to change the chemical makeup of a rock's surface so that the hydrocarbon phase that is being produced can flow more efficiently. In the case of the North Field, the hydrocarbon phase being produced is gas. Tang and Firoozabadi (2000) used FC-722 to change the chemical makeup of a rock's surface. FC-722 is a fluoropolymer-type chemical that is colorless, soluble only in a specific fluoro-solvent, and expensive. The chemical structure of FC-722 is made up of a fluorochemical group, a silanol group, and an anionic group. The fluorochemical group repels water and

oil, while the anionic and silanol groups chemically bond onto rock surfaces resulting in a durable treatment (Tang and Firoozabadi 2000). Fig. 15 shows a case where a reservoir is initially oil-wet. Then after a certain period, chemicals are injected into the wellbore, the chemical diffuses radially into the reservoir, a chemical process takes place on the surface of the rock, and the wettability of the reservoir is permanently changed.

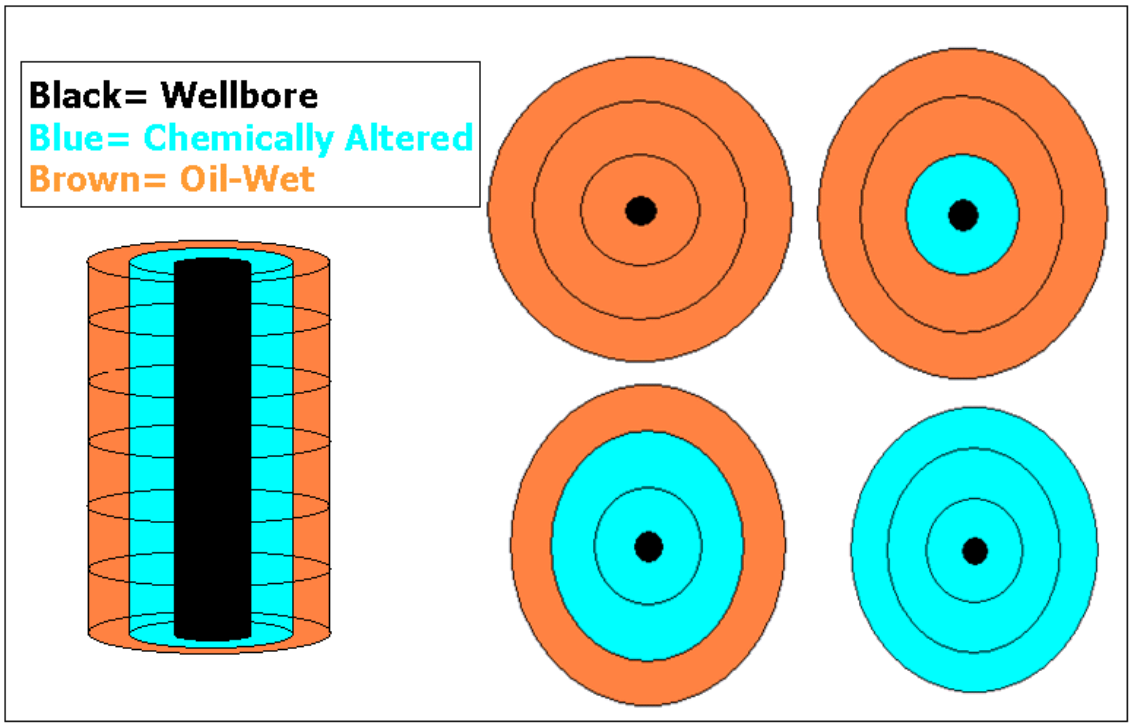

Fig. 15: Radial Diffusion

3.5. Field Application

Tang and Firoozabadi (2000) found that wettability alteration has a significant effect on both gas and oil relative permeability. This thesis will simulate wettability alteration by using two different relative permeability tables to model wettability

alteration in the North Field. One simulation will be run with relative permeability data (Table 11) from an oil wet reservoir, and one simulation will be run with relative permeability data (Table 12) from an intermediate wet reservoir. Table 11 describes an untreated reservoir since no chemical treatment has been applied to change the original oil wet relative permeability. A combination of oil wet permeability data and intermediate wet permeability data will be incorporated into a few cases to model various chemical injection volumes.

Table 11: Oil Wet Relative Permeability Data

Gas Saturation	Relative Permeability (Gas)	Oil Saturation	Relative Permeability (Oil)
.425	0	.412	0
.442	.021	.44	.008
.491	.094	.509	.024
.563	.267	.604	.050
.591	.348	.662	.077
.623	.452	.763	.156
.712	.776	.818	.222
		.85	.274

Table 12 shows intermediate wet relative permeability that has been altered from the Table 11 permeability data by injecting a chemical with 2% FC-722.

Table 12: Intermediate Wet Relative Permeability Data

Gas Saturation	Relative Permeability (Gas)	Oil Saturation	Relative Permeability (Oil)
.372	0	.065	0
.414	.014	.157	.001
.497	.073	.241	.041
.542	.107	.312	.075
.612	.193	.394	.130
.688	.300	.454	.178
.768	.431	.500	.220
.841	.595	.546	.262
.933	.807	.590	.307
		.620	.341
		.672	.399
		.729	.472
		.818	.599

Using permeability data from Table 11 and Table 12, a simulation was run in order to determine the effect wettability alteration has on block oil saturation in the near-wellbore region. Figs. 16 through Fig. 18 show what occurs when a reservoir undergoes wettability alteration. Each simulation is run at a constant gas rate production of 125,000 Mscf/day gas rate upper limit. Fig. 16 shows a block oil saturation comparison between a reservoir that has been untreated, and a reservoir that has been treated with the FC-722 chemical. Fig. 16 shows that when the reservoir changes from oil wet (red curve) to intermediate wet (green curve), the oil saturation in the completion-region grid blocks is reduced significantly (yellow area) from saturation values of around 0.50 to saturation values of around 0.25.

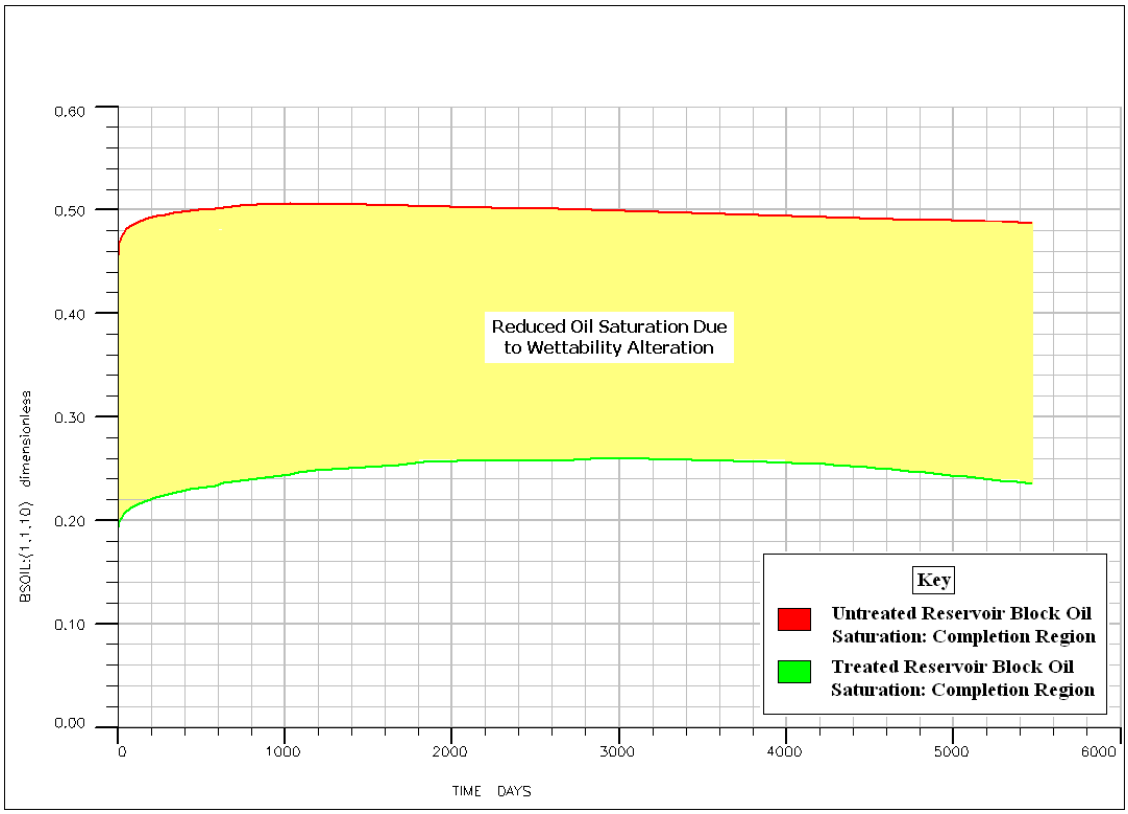

Fig. 16: Wettability Alteration Oil Saturation Comparison

Even though the well is initially set to a constant production rate of 125,000 Mscf/day, the rate will eventually decline below 125,000 Mscf/day. This decline in the gas production rate occurs after the bottom hole pressure of 2500 psi is reached. Once 2500 psi has been reached, the bottom hole pressure becomes the controlling production factor, and the gas production rate starts to decrease. In Fig. 17, the switch from a gas rate control limit to a bottom hole control limit occurs when the untreated reservoir curve (blue line) starts becoming non-linear around 1,035 days. Fig. 17 shows the increased total gas production that occurs when a reservoir is chemically treated so that the entire reservoir switches from an oil wet reservoir to an intermediate wet reservoir.

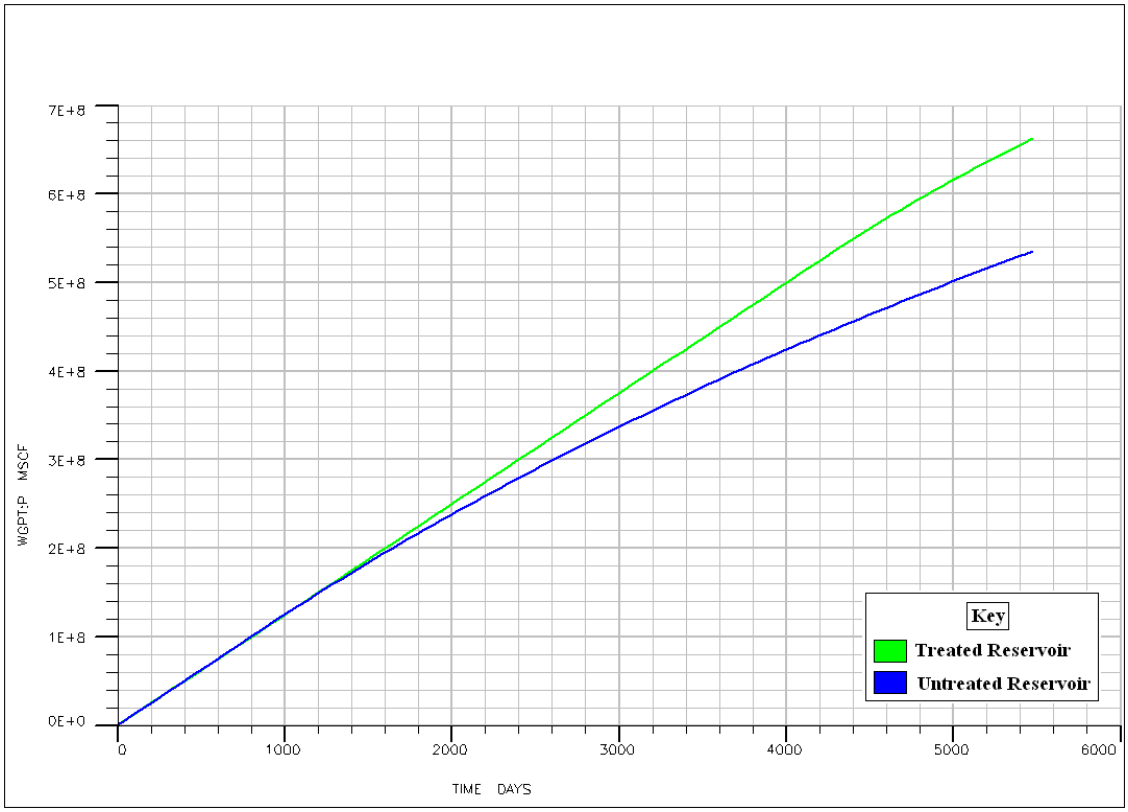

Fig. 17: Wettability Alteration Total Gas Production Comparison

Fig. 18 plots total gas production curves for a reservoir that has been injected with different pore volumes of FC-722. Fig. 18 shows that the best case for total gas production occurs when the entire radius of the reservoir (4,140 ft) is injected with FC-722. However, in the field, this may not be practical due to the large volume of chemical that would be needed. Various geologic barriers might also prevent the chemical injection from extending the intended distance into the reservoir.

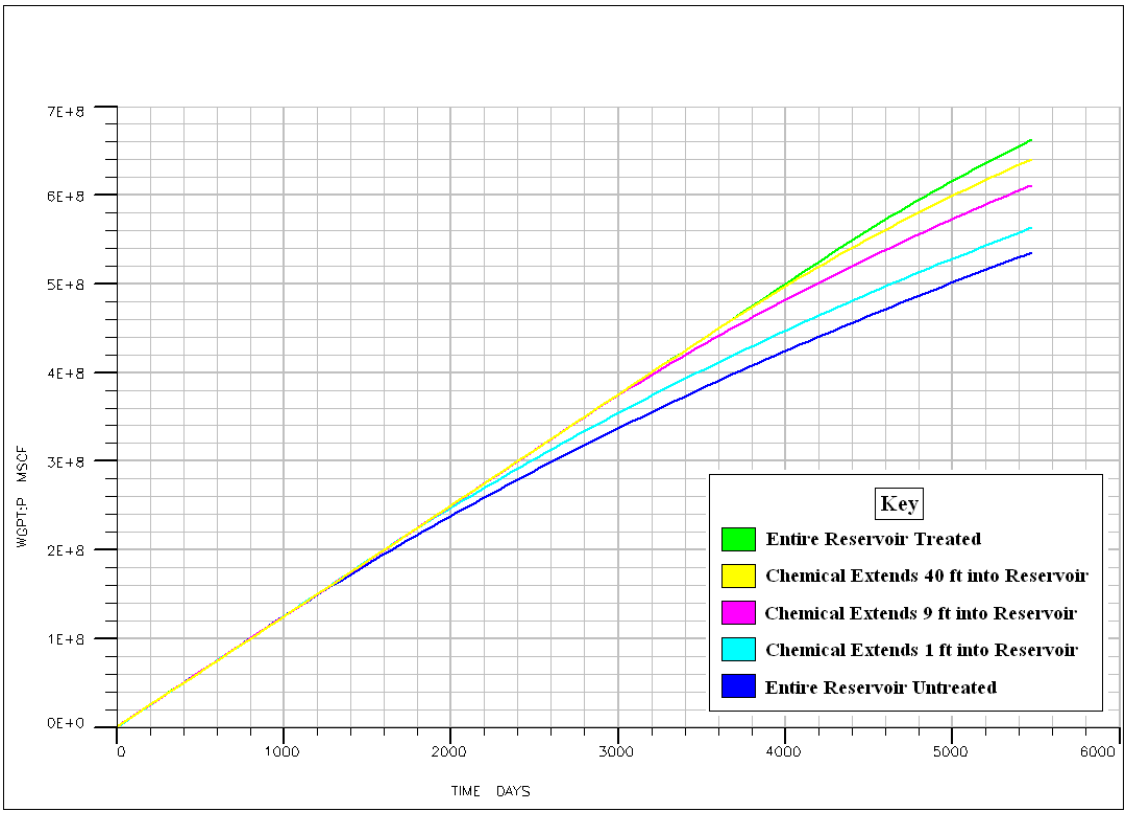

Fig. 18: Various Wettability Alteration Effects

Table 13 shows the total volume of chemical that would be need to be injected in order to chemically alter: the entire reservoir (treated), 40 ft of the reservoir, 9 ft of the reservoir, 1 ft of the reservoir, and 0 ft of the reservoir (untreated). As seen in Table 13, trying to chemically alter the entire reservoir pore volume of 9,254,235,012 scf would be extremely difficult due to the volume of FC-722 (370,169,401 scf) that would be required. However, injecting a FC-722 pore volume to extend 9 ft (1,749 scf) into the reservoir might be a more realistic field application.

Table 13: Reservoir Treatment

Treatment Type	Pore Volume (scf)	Chemical Needed 2 X Pore Volume (scf)	FC-722 (2%) Pore Volume (scf)
Reservoir Untreated	0	0	0
Chemical Extends 1 ft into Reservoir	540	1080	21.6
Chemical Extends 9 ft into Reservoir	43,735	87,470	1,749
Chemical Extends 40 ft into Reservoir	863,893	1,727,786	34,556
Entire Reservoir Treated	9,254,235,012	18,508,470,024	370,169,401

Table 14 shows that an additional 76,000,000 Mscf of gas production can be achieved after 15 years if the chemical is injected 9 ft into the reservoir compared to an untreated reservoir.

Table 14: Wettability Alteration Impact on Total Gas Production in North Field

Treatment Type	5 Year Total Gas Production (Mscf)	10 Year Total Gas Production (Mscf)	15 Year Total Gas Production (Mscf)
Reservoir Untreated	2.20E 8	3.89E 8	5.35E 8
Chemical Extends 1 ft into Reservoir	2.27E 8	4.16E 8	5.63E 8
Chemical Extends 9 ft into Reservoir	2.28E 8	4.46E 8	6.11E 8
Chemical Extends 40 ft into Reservoir	2.29E 8	4.57E 8	6.41E 8
Entire Reservoir Treated	2.29E 8	4.57E 8	6.63E 8

Table 15 shows the added value wettability alteration can create for a single well model in the North Field over a 15 year period. Table 15 shows that if a $6/Mscf market value is assumed, then wettability alteration could increase the gas production revenue by $168 million for a 1 ft injection, $456 million for a 9 ft injection, and $636 million for

a 40 ft injection over a 15 year period. The cost due to the chemical injection of FC-722 is expected to be a small percentage of the added value that would result from wettability alteration effects.

Table 15: Wettability Alteration Added Value to North Field

Treatment Type	Market Value ($/Mscf)	5 Year Added Value ($ million)	10 Year Added Value ($ million)	15 Year Added Value ($ million)
Reservoir Untreated	$6.00	0	0	0
Chemical Extends 1 ft into Reservoir	$6.00	$42	$162	$168
Chemical Extends 9 ft into Reservoir	$6.00	$48	$342	$456
Chemical Extends 40 ft into Reservoir	$6.00	$54	$408	$636
Entire Reservoir Treated	$6.00	$54	$408	$768

3.6. Summary

Li and Firoozabadi (April 2000) have shown that a permanent intermediate gas wetting can be established in Berea core samples through chemical treatment. Based on this result from Li and Firoozabadi (April 2000), and relative permeability data taken from Tang and Firoozabadi (2000), this section explored a North Field application of wettability alteration and found the following:

- Wettability alteration significantly decreases block oil saturation in the near-completion region of the wellbore. This is a major reason as to why the total gas production subsequently increases after wettability alteration takes affect.

- Assuming a reservoir is initially oil-wet, simulation results show that total gas production could be maximized if a reservoir could be entirely treated with FC-722 so that the entire reservoir would become intermediate wet.

- Changing the wettability of an entire reservoir may be unrealistic due to the volume of chemical required and the distance away from the wellbore to where the chemical would need to reach in the reservoir. Table 15 summarizes the added value that could be achieved in the North Field due to wettability alteration.

4. APPLICATION OF HORIZONTAL WELLS IN THE NORTH FIELD

4.1. Overview

This section uses a horizontal well model developed from North Field reservoir data provided in section 2 in order to study the idea that a horizontal well can reduce condensate blockage more than a vertical well, and thereby increase total gas production. The horizontal well model used in this section is based off the multilateral well model defined in detail in Section 2 of this thesis.

4.2. Drawdown Pressure Comparison in the North Field

Fig. 19 shows a drawdown comparison between a vertical well and a horizontal well. The red line shows the average reservoir pressure for both the horizontal well and the vertical well. The average reservoir pressure begins at around 5,260 psia and drops to around 5,100 psia after 15 years (5,475 days). The green line shows the flowing bottom hole pressure for the horizontal well, and the blue line shows the flowing bottom hole pressure for the vertical well. Drawdown is defined as the difference between the average reservoir pressure and the flowing bottom hole pressure (Schlumberger 2009). Fig. 19 shows that the drawdown pressure for the vertical well is much larger than the drawdown pressure for the horizontal well.

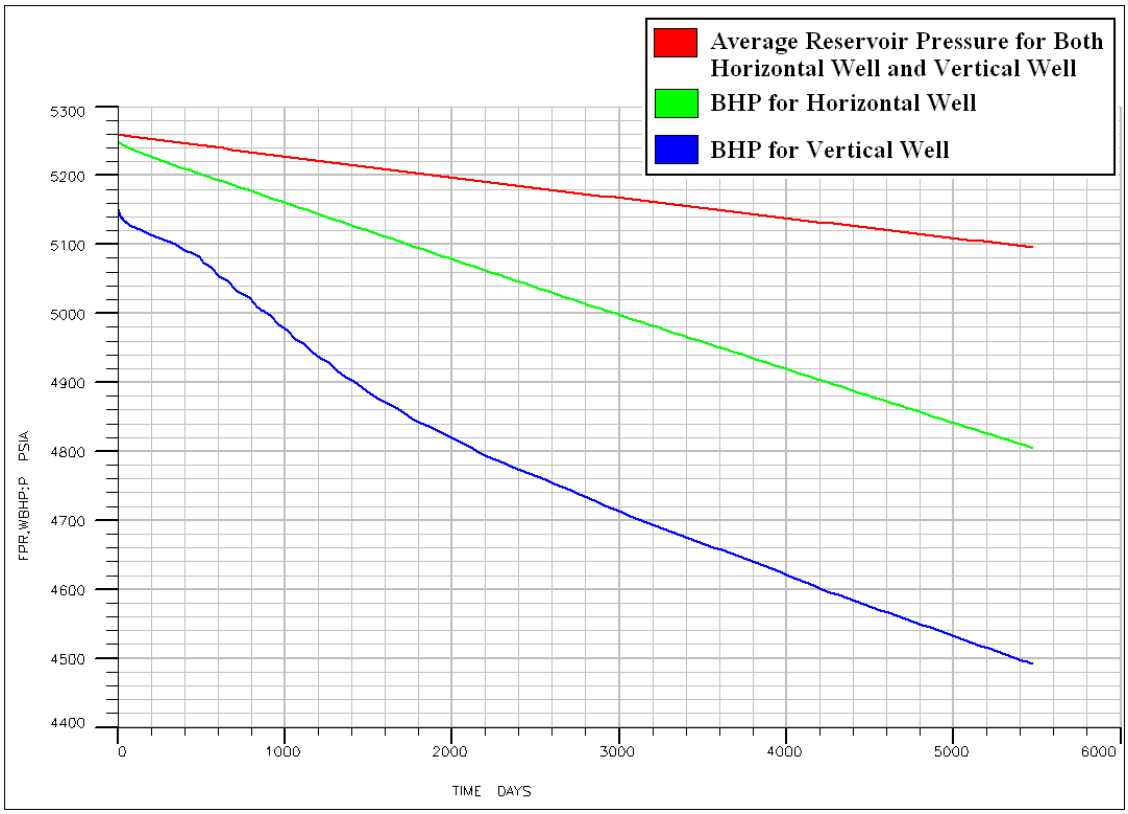

Fig. 19: Vertical Well and Horizontal Well Pressure Drawdown Comparison

4.3. Oil Saturation Comparison in the North Field

The large drawdown pressure for the vertical well (Fig. 19) is a major reason why block oil saturation (condensate blockage) forms on a much larger scale (6.5 times) for the vertical well (0.26) than the horizontal well (0.04) as seen in Fig. 20. The large pressure drawdown for the vertical well causes the dew point to be reached at a much earlier time for the vertical well (400 days) than the horizontal well (1,880 days). Fig. 20 shows that once the dew point pressure is reached, oil saturation begins to form in the near wellbore region. The near wellbore region is defined as the thickness of the grid block closest to the wellbore in the high-perm completion layer. For the vertical well, the

thickness of the grid block closest to the wellbore is 0.25 ft, and the high-perm completion layer is layer 112 (z-coordinate). For the horizontal well, the thickness of the grid block closest to the wellbore is 1.92 ft, and the high-perm completion layer is layer 15 (y-coordinate).

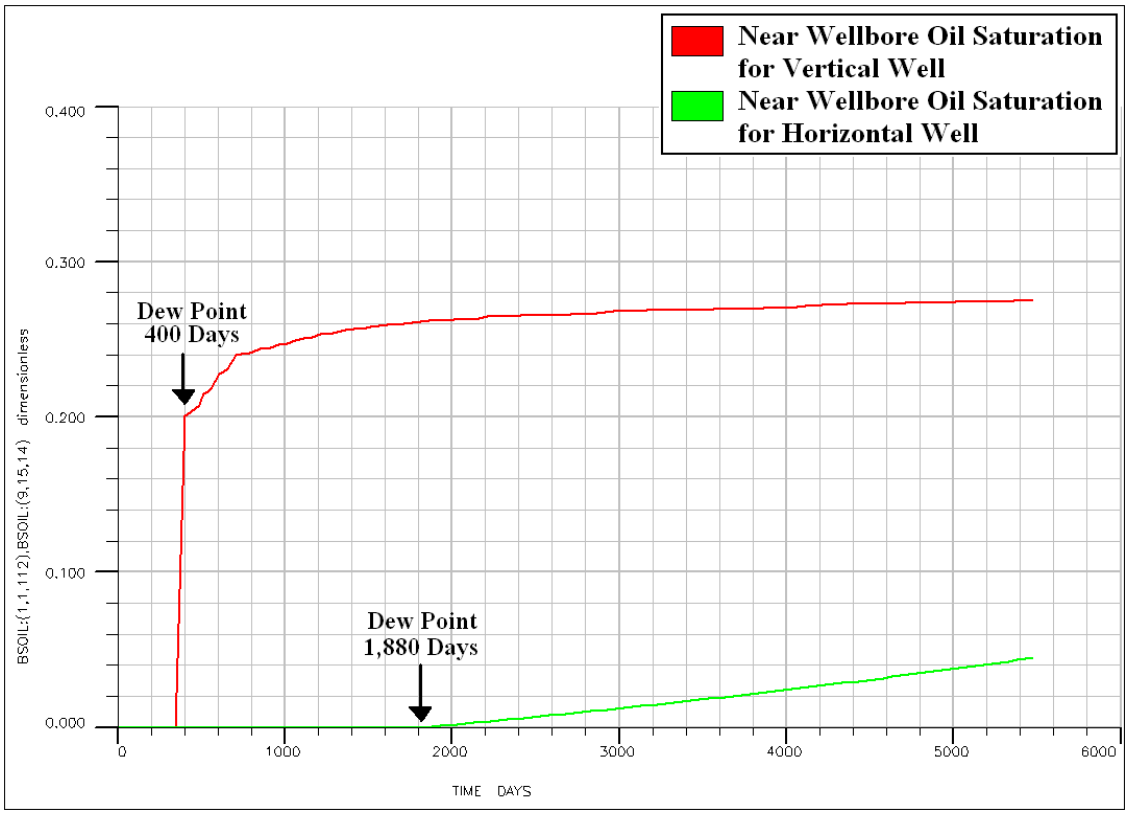

Fig. 20: Oil Saturation Comparison

4.4. Productivity Index

The productivity index describes the degree of communication between a well and the reservoir, and can be calculated from field measurements. The productivity index, or PI, will vary with the fluid mobilities at the well. For steady-state conditions,

the productivity index is defined as the production rate of a chosen phase divided by the drawdown. The productivity index for a horizontal well can be calculated by Eq. (4.1):

$$J = \frac{Q_p}{P_d - P_w} \tag{4.1}$$

J is productivity index, Q_p is the production rate of the chosen phase, P_d is the pressure at the drainage radius, and P_w is the bottom hole pressure. The productivity index for the vertical well can be calculated by Eq. (4.2):

$$J = \sum_j [T_{wj} M_{pj} (\frac{\ln(r_o / r_w) + s}{\ln(r_d / r_w) + s})] \tag{4.2}$$

T_{wj} is the well connection factor, M_{pj} is the phase molar mobility, r_o is the pressure equivalent radius, r_w is the well radius, r_d is the drainage radius, and s is the skin factor. Eq. (4.2) can not be used to calculate the productivity index for a horizontal well because the equation requires that a steady radial flow regime perpendicular to the well bore exists out to the drainage radius. The flow regime in a horizontal well is disrupted by the top and bottom boundaries of the formation and the ultimate flow regime is no longer radial, but rather linear or pseudo-radial.

4.5. North Field Productivity Index Comparison

Fig. 21 shows that the productivity index (PI) for the horizontal well is much higher than the productivity index for the vertical well.

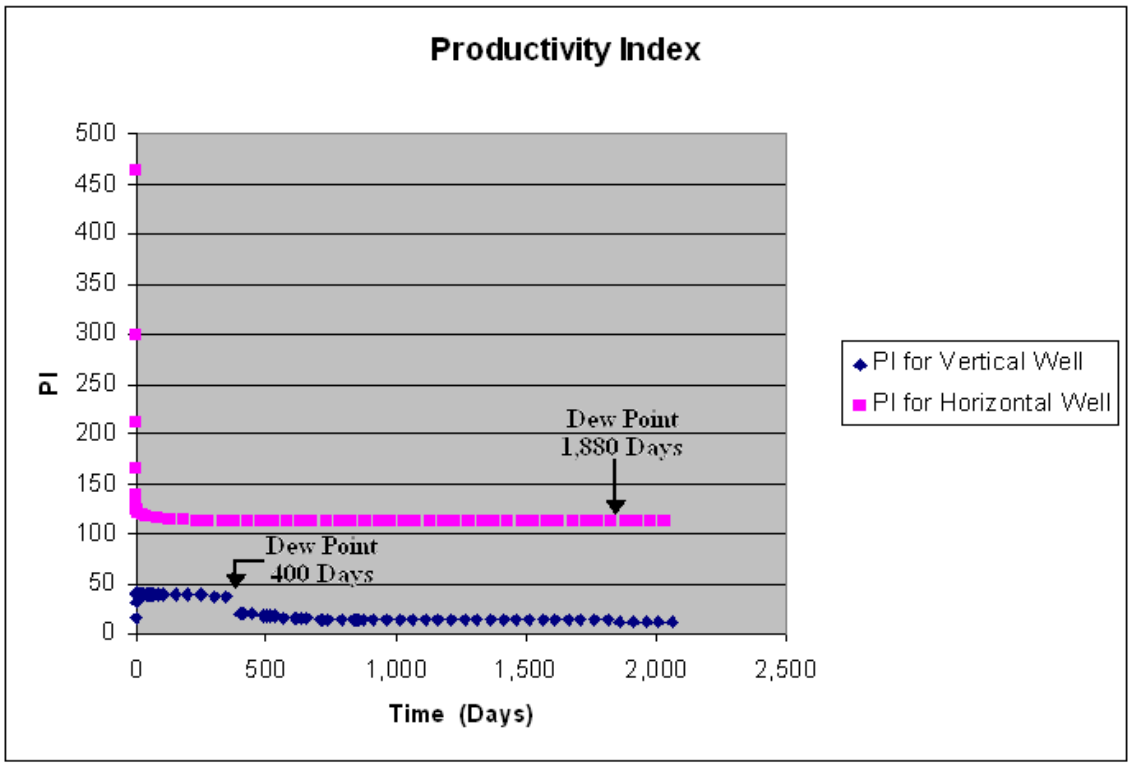

Fig. 21: Productivity Index Comparison

The dew point for the vertical well occurs at 400 days and the dew point for the horizontal well occurs at 1,880 days. Fig. 21 shows that the PI decreases sharply (37 to 19) when the dew point is reached in the vertical well. The PI for the horizontal well was not affected by the dew point since the PI is 111 before the dew point pressure is reached, and remains at 111 after the pressure drops below the dew point. Table 16 shows these results.

Table 16: Productivity Index

	Before Dew Point	After Dew Point
Horizontal Well PI (Mscf/psia)	111	111
Vertical Well PI (Mscf/psia)	37	19

When compared with vertical wells, horizontal wells provide increased productivity because there is a larger wellbore surface area in the net pay layer as seen in the figure on page 69 of Section 5. However, Fig. 21 also shows that part of the productivity increase resulting from a horizontal well is due to the ability of a horizontal well to decrease condensate saturation in the near wellbore. Table 17 shows that the horizontal well is able to increase the productivity 1.9 times more than a vertical well due to a reduction in condensate blockage.

Table 17: Productivity Increase Due to Condensate Blockage Reduction

Ratio	Before Dew Point	After Dew Point	Added Value Due to Reduced Condensate Blockage
$\frac{\text{(Horizontal PI)}}{\text{(Vertical PI)}}$	3.0	5.8	1.9

4.6. Summary

This section used a horizontal well model (based off multilateral well model described in section 2) in order to study the idea that a horizontal well has a smaller drawdown pressure than a vertical well. This smaller drawdown pressure in the horizontal well leads to a delayed dew point pressure being reached compared with the vertical well. Once the dew point pressure is reached and oil saturation forms in the reservoir, the magnitude of oil saturation buildup in the near wellbore is 6.5 times lower in the horizontal well than the vertical well. The ratio of horizontal well PI to vertical well PI is 3 before the dew point and 5.8 after the dew point. The fact that the PI increased from 3 before the dew point to 5.8 after the dew point indicates that the increase in productivity index (1.9 times) is directly due to the ability of the horizontal well to reduce condensate blockage in the near wellbore. The PI in the vertical well case is affected negatively once the dew point pressure is reached, while the PI in the horizontal well seems to remain steady even after the dew point pressure is reached.

5. NON DARCY FLOW EFFECTS IN HORIZONTAL WELLS IN THE NORTH FIELD

5.1. Non Darcy Effects

5.1.1. Non Darcy Equation

Darcy's law is used to describe the horizontal flow of fluids through a porous medium. In order for Darcy's law to apply, the fluid velocity must be at low or moderate rates. For radial flow, Darcy's law states that the pressure drop in the direction of flow is proportional to the velocity of the fluid, or:

$$\frac{dp}{dr} = \frac{\mu}{k} \bullet v \qquad (5.1)$$

where:

$\frac{dp}{dr}$ = Pressure Gradient

μ = Viscosity

k = Permeability

v = Superficial Velocity

The right side of Eq. (5.1) is called a viscous force component. As flow rates become higher, Eq. (5.1) can no longer accurately describe fluid flow because of a newly created inertial force which acts on fluids within the porous medium. This new inertial force comes into existence because of convective accelerations of the fluid particles as they pass through pore spaces at high flow rates. For this case, Forchheimer added the following inertial force term: $\beta \bullet \rho \bullet v^2$

where:

$\beta =$ Non Darcy Coefficient

$\rho =$ Fluid Density

$v =$ Superficial Velocity

When the term $\beta \bullet \rho \bullet v^2$ is added to Eq. (5.1), the following flow equation is obtained,

$$\frac{dp}{dr} = \frac{\mu}{k} \bullet v + \beta \bullet \rho \bullet v^2 \qquad (5.2)$$

In the past, the β has been called turbulence factor, coefficient of inertial resistance, velocity coefficient, Forchheimer coefficient, inertial coefficient, beta factor and Non Darcy Coefficient (Dacun and Engler 2001). As seen from Eq. (5.2), when superficial velocity is low, the inertial force term approaches zero and can therefore be discarded (Dake 1978).

5.1.2. Literature Review on Non Darcy Flow

Tek *et al*. (1961) derived a partial differential equation to represent fluid flow through porous media at all rates. They numerically solved the equation so that isochronal back-pressure curves could be constructed. Their calculations indicated that the drainage radius for a gas well in turbulent flow depended on the rate of production at the wellbore. Based on experimental data, dimensional analysis, and physical considerations, Geertsma (1959) introduced the following empirical relationship between the inertial coefficient and permeability and porosity:

$$\frac{\beta \phi^{5.5}}{\sqrt{a}} = 0.005 \qquad (5.3)$$

This equation is only valid for 100% liquid or 100% gas saturation since gas flow combined with liquid saturation have much higher inertial coefficients compared to the dry state. Phipps and Khalil (1975) proposed a direct method to solve for the parameters, a, b, and n in the following Forchheimer-type equation:

$$\frac{\Delta p}{\Delta L} = au + bu^n \qquad (5.4)$$

a and b are constants for a particular porous media and n is the velocity exponent. This equation is the exact same as Eq. (5.2) when n=2. Evans *et al.*(1985) investigated the effects of immobile liquid saturations on the Non Darcy flow coefficient. They found that the Non Darcy flow coefficient increases with decreased permeability, decreased porosity, and increased liquid saturation. They developed a correlation between the Non Darcy flow coefficient, permeability, porosity, immobile liquid saturation, fluid properties, and effective stress. Jones (1987) developed a multi-layer flow model to show that the departure between the $\beta k\phi$ (Reynolds number dimension length) and the $\sqrt{\frac{k}{\phi}}$ term is due to the non-linear dependence of inertial resistance on permeability variation in a core plug. Firoozabadi *et al.* (1992) found that: gas property effects do not account for high-velocity flow in porous media, Darcy's law does not sufficiently represent high-velocity flow, and the Non Darcy flow coefficient is a function of rock properties that is independent of length. They further stated that the squared-gradient term in the flow equation does not adequately replace high-velocity mechanisms. Al-Rumhy and Kalam (1993) investigated the effects of liquid saturations on the Non Darcy coefficient. They found that gas slippage correction is crucial in determining the inertial resistance coefficients from high rate gas flow data. They also concluded that Non Darcy

coefficients greatly increase when mobile and immobile fluid saturations are present. Frederick and Graves (1994) used 407 data points from 24 cores to develop empirical correlations which relate the Non Darcy flow coefficient to permeability, porosity, and water saturation. They concluded that saturation does influence the Non Darcy flow coefficient and that their correlations can be used in multiphase flow calculations.

5.1.3. Non Darcy Correlations

Table 18 shows the various 1-phase correlations that can be used to obtain a Non Darcy flow coefficient.

Table 18: Single-Phase Correlations for the Non Darcy Coefficient

1-Phase Correlation	Forchheimer Number
Jones	9.81
Dake	20.06
Liu	28.10
Thauvin and Mohanty	35.83

Each correlation gives different Non Darcy flow coefficients which are converted to Forchheimer units by multiplying by 1.01325E6 1/cm. The Forchheimer unit is then input into the simulator, and the simulation run is initiated. Dake (1978) used a laboratory determined relationship between beta and absolute permeability to obtain the following correlation:

$$\beta = \frac{2.73x10^{10}}{k^{1.1045}} \qquad (5.5)$$

Jones (1987) carried out experiments on 355 sandstone and 29 limestone cores with the following core types: fine-grained sandstone, crystalline limestone, and vuggy limestone. From his experiments, he obtained the following correlation:

$$\beta = \frac{6.15x10^{10}}{k^{1.55}} \tag{5.6}$$

Eq. (5.5) and Eq. (5.6) use only one variable (permeability) to obtain a Non Darcy flow coefficient. Liu *et al.* (1995) analyzed work done by Geertsma, Cornell, Katz, Evans, and Whitney, and developed the following correlation:

$$\beta = 8.91x10^{8} \bullet k^{-1} \bullet \phi^{-1} \bullet \tau \tag{5.7}$$

Liu *et al.* (1995) considered the effects of porous medium tortuosity, τ, on the Non Darcy coefficient and included porosity as a variable. Thauvin and Mohanty (1998) developed the following Non Darcy coefficient correlation:

$$\beta = \frac{1.55x10^{4} \bullet \tau^{3.35}}{k^{0.98} \bullet \phi^{0.29}} \tag{5.8}$$

They created a pore-level network model to describe high velocity flow. Fig. 22 shows the effect these various correlations have on total gas production in the vertical well model. In this thesis, the Non Darcy coefficient was converted into a Forchheimer number of 20.06 (Table 18), and was then used to study Non Darcy effects in vertical and multilateral wells. Fig. 22 shows that total gas production is slightly impacted by various Non Darcy coefficients (Table 18).

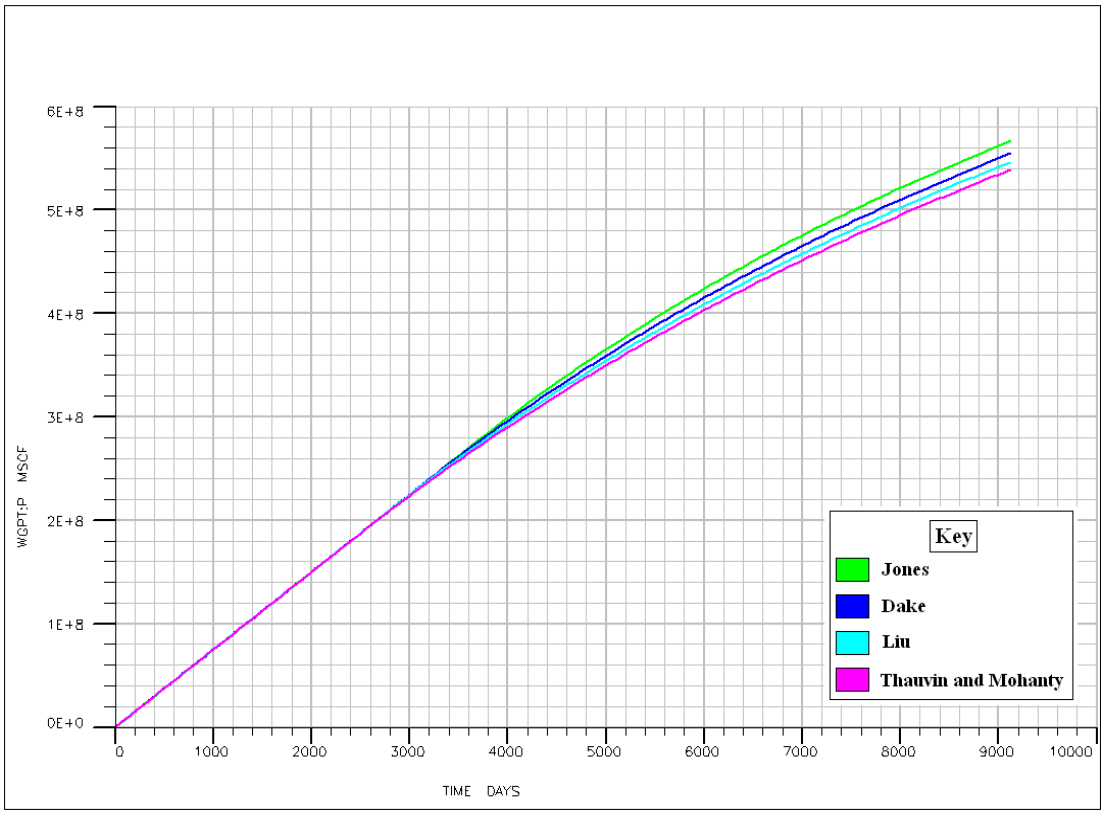

Fig. 22: Impact of Non Darcy Flow Correlations on Total Gas Production in a Vertical Well

5.1.4. Non Darcy Sensitivity

Once the Dake (1978) correlation was chosen, a Non Darcy coefficient sensitivity study was completed to further determine the relationship between the Non Darcy coefficient and total gas production. Table 19 shows the Non Darcy coefficients used to carry out the sensitivity study. A base Non Darcy coefficient of 20.06 was used as a constant, and then this constant was increased and decreased by various percentages to test the impact this change would have on total gas production.

Table 19: Non Darcy Coefficient Sensitivity on Gas Production

Decrease 50%	Decrease 10%	Base	Increase 10%	Increase 50%
10.03	18.054	20.06	22.066	30.09

Fig. 23 shows the simulation results of the Non Darcy coefficients defined in Table 19. Fig. 23 shows that larger changes in the Non Darcy coefficient, leads to larger changes in total gas production in a vertical well.

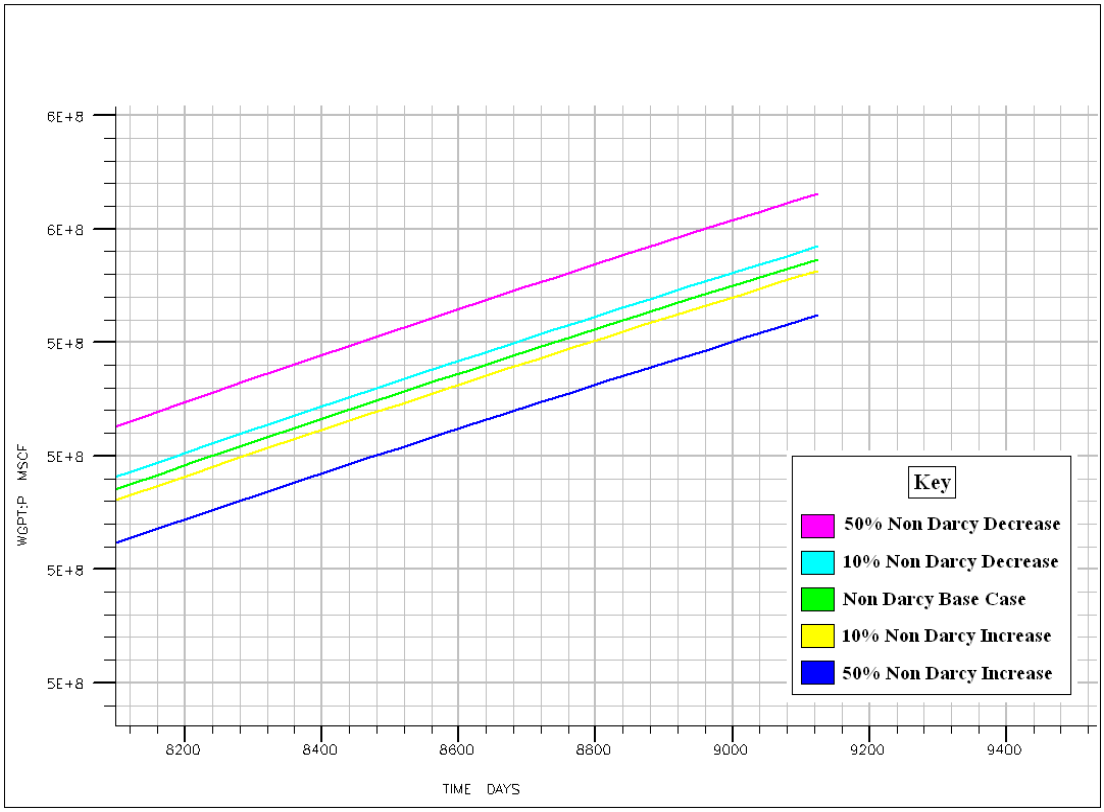

Fig. 23: Sensitivity of Non Darcy Effects on Total Gas Production in a Vertical Well

5.1.5. Comparison of Non Darcy Effects in Vertical and Multilateral Wells

Fig. 24 shows Non Darcy effects in vertical and multilateral wells at a limiting gas rate of 75,000 Mscf/day. A limiting gas rate of 75,000 Mscf/day was chosen based on previous work done in the North Field (Whitson and Kuntadi 2005). The pink and light blue curves show the base cases for the multilateral and vertical well models, respectively. The green curve shows that Non Darcy effects decrease the gas production total from the vertical well base case. The dark blue curve is hidden under the base case for the multilateral well model since Non Darcy effects have little impact on total gas production for the multilateral well at a rate of 75,000 Mscf/day. Fig. 25 shows why Non Darcy effects do not appear in a multilateral well in the North Field. The figure on the left (a) shows the completion area for the high permeability region in the K1 layer of the vertical well. The figure on the right (b) shows the completion area for the high permeability region in the K1 layer of the horizontal well. Fig. 25 shows that the area completed for the vertical well (11.89 ft^2) is much smaller than the area completed for the horizontal well (546.6 ft^2).

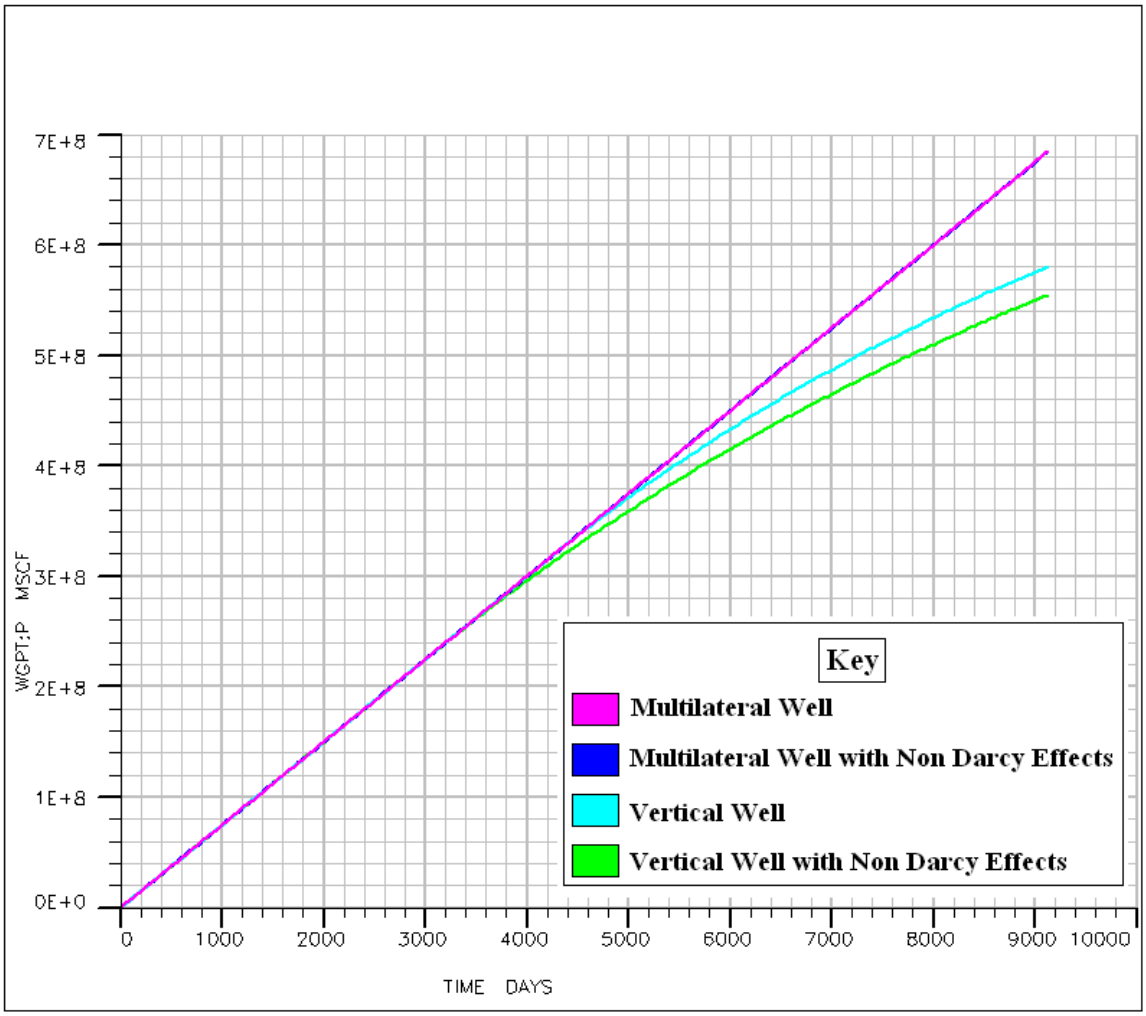

Fig. 24: Non Darcy Effects on Vertical and Multilateral Well Total Gas Production at 75,000 Mscf/day

Eq. (5.9) further explains how this impacts velocity.

$$Q = VA \tag{5.9}$$

Q is flow rate, V is velocity, and A is area. The flow rate remains constant (75,000 Mscf/day) for both the vertical well and the horizontal well, but the area is larger for the horizontal well. This means that the velocity in the horizontal well (137, 211 ft/day) will be 46 times less than the velocity in the vertical well (6,307,821 ft/day). We know from the last term in Eq. (5.2) that the Non Darcy effect becomes negligible as velocity becomes small.

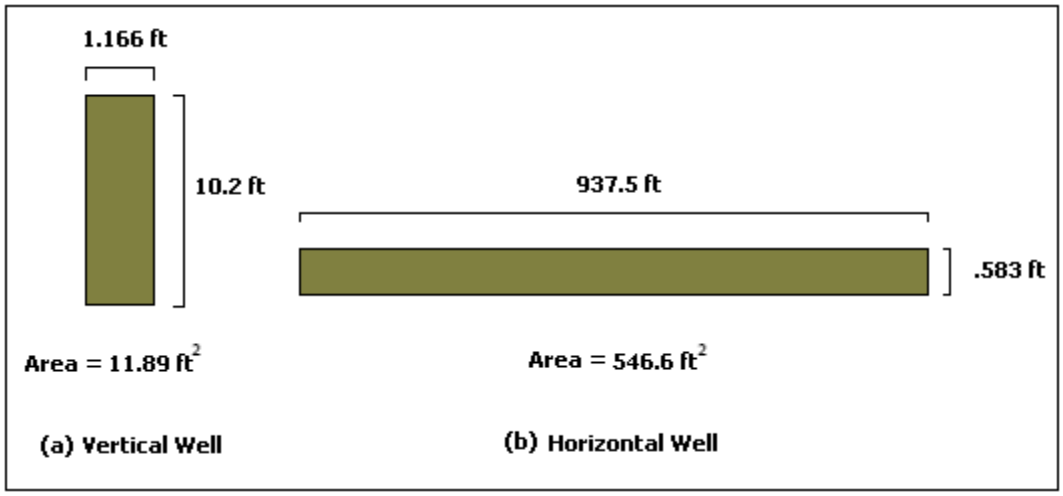

Fig. 25: Flow Rate Surface Area Comparison

5.1.6. Non Darcy Effects on Total Gas Production

The Dake (1978) correlation was used to model Non Darcy effects. Fig. 26 shows that when Non Darcy effects can be minimized, or reduced to zero, total gas production can be increased. Total gas production without Non Darcy effects is 25 MMscf more that

total gas production with Non Darcy effects at the end of 25 years. This means that Non Darcy flow decreases total gas production in the North Field by 4.5% after 25 years.

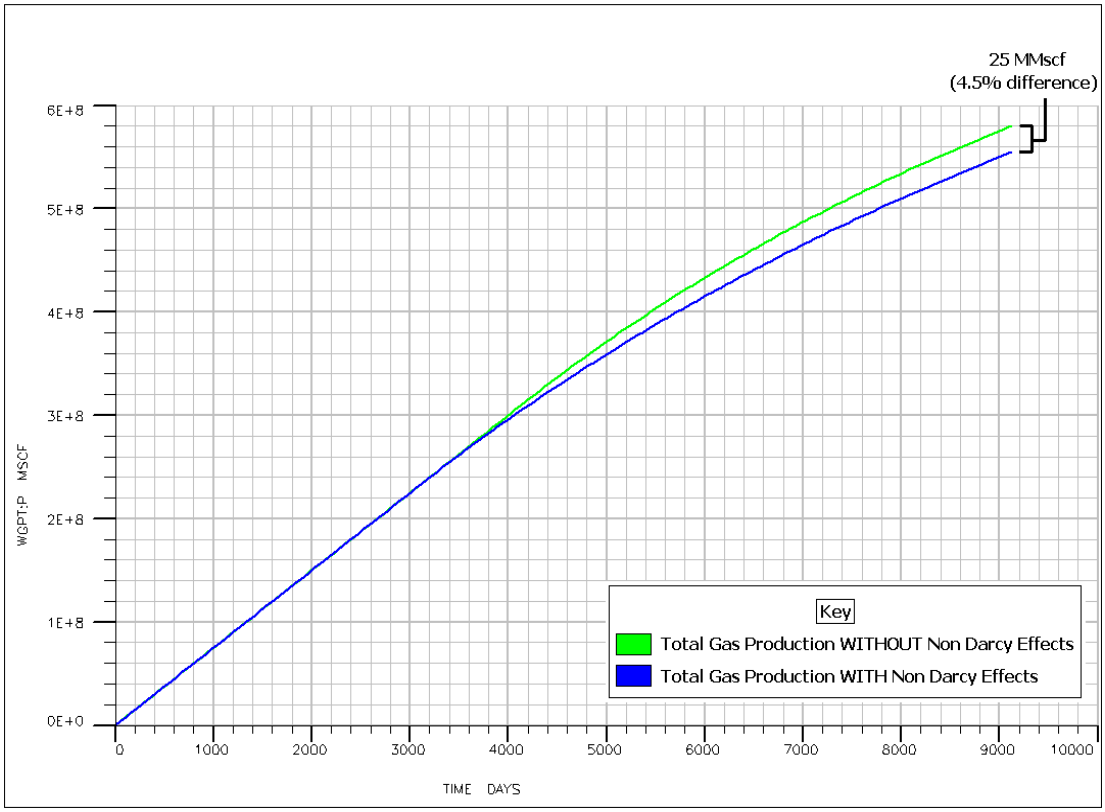

Fig. 26: Non Darcy Effects on Total Gas Production

5.2. Summary

The Dake (1978) correlation was chosen to model Non Darcy flow. It was found that Non Darcy flow had a negative impact on gas production in the vertical well model, but had little impact on the multilateral well model. The reason Non Darcy flow had little impact on the multilateral well was due to a larger wellbore surface area being exposed in the reservoir. This larger wellbore area exposure in the reservoir, caused a

decrease in gas velocity, which forced the Non Darcy term (last term) in Eq. (5.2) to approach a negligible value. Results also showed that larger changes in the Non Darcy coefficient, lead to larger changes in the total gas production in a vertical well. Non Darcy flow decreased total gas production in the North Field by 4.5% after 25 years.

6. CONCLUSIONS

6.1. Summary

Eclipse DATA files were created to model a vertical well in radial coordinates, and horizontal/multilateral wells in Cartesian coordinates. Based off the work done by Li and Firoozabadi (April 2000), a North Field simulation study on wettability alteration was completed in section 3. Results showed that wettability alteration significantly decreases block oil saturation in the near-completion region of the wellbore. This is a major reason as to why the total gas production subsequently increases after wettability alteration takes effect. Results also showed that total gas production is maximized if a reservoir is entirely treated with FC-722 so that the entire reservoir is intermediate wet. However, a more realistic field injection case involves injecting 1,749 scf of FC-722 into the North Field reservoir. This would allow chemical alteration to take effect up to 9 ft away from the wellbore, and add $456,000,000 worth of value to a single well in the North Field after 15 years of production. When comparing horizontal wells and vertical wells in section 4, it was found that smaller drawdown pressures in the horizontal well led to a delayed dew point pressure being reached. Once the dew point pressure was reached and oil saturation formed in the reservoir, the magnitude of oil saturation buildup in the near wellbore was 6.5 times lower in the horizontal well than the vertical well. It was also found that the productivity index increased 1.9 times as a result of condensate blockage reduction in a horizontal well. While examining Non Darcy effects in section 5, it was found that multilateral wells did not seem to be impacted by Non Darcy effects at a maximum flow rate of 75,000 Mscf/day. It was found that decreased

fluid velocity in horizontal wells was a major reason for negligible Non Darcy effects in North Field horizontal wells. Various Non Darcy correlations were studied including correlations by Jones (1987), Dake (1978), Liu *et al*. (1995), and Thauvin and Mohanty (1998). The Dake (1978) correlation was the correlation was used to study Non Darcy effects in this paper. A Non Darcy sensitivity study was completed which showed that larger changes in the Non Darcy coefficient lead to larger changes in total gas production. It was also found that Non Darcy flow decreased total gas production in a North Field vertical well by 4.5% after 25 years.

6.2. Future Work

- Further analysis could be done if field data could be obtained to give needed Non Darcy variables.
- Further analysis could be done if lab experiments could be performed to give needed Non Darcy variables.
- Intelligent well valves and chokes can now be incorporated into the horizontal and multilateral well models.
- More accurate simulations could be achieved in the multilateral well case if more (smaller) grid blocks were used. However, the A&M Eclipse simulation license has a limit on the number of grid blocks that can be used to study a reservoir.

REFERENCES

Afidick, D., Kaczorowski, N., and Bette, S. (1984). Production Performance of a Retrograde Gas Reservoir: A Case Study of the Arun Field. Paper SPE 28749 presented at the SPE Asia Pacific Oil & Gas Conference, Melbourne, Australia, 7-10 November.

Ahmed, T., Evans, J., Kwan, R., and Vivian, T. (1998). Wellbore Liquid Blockage in Gas-Condensate Reservoirs. Paper SPE 51050 presented at the SPE Eastern Regional Meeting, Pittsburgh, Pennsylvania, 9-11 November.

Al-Anazi, H., Xiao, J., Al-Eidan, A., Buhidma, I., Ahmed, M., Al-Faifi, M., and Assiri, W. (2007). Gas Productivity Enhancement by Wettability Alteration of Gas-Condensate Reservoirs. Paper SPE 107493 presented at European Formation Damage Conference, Scheveningen, The Netherlands, 20 May-1 June.

Ali, J., Butler, S., Allen, L., and Wardle, P. (1993). The Influence of Interfacial Tension on Liquid Mobility in Gas Condensate Systems. Paper SPE 26783 presented at the SPE Offshore European Conference, Aberdeen, Scotland, 7-10 September.

Al-Rumhy, M., and Kalam, M. (1993). Relationship of Core-Scale Heterogeneity with Non Darcy Flow Coefficients. Paper SPE 25649 presented at SPE Middle East Technical Conference and Exhibition, Kingdom of Bahrain, 3-6 April.

Al-Shammasi, A., and D'Ambrosio, A. (2003). Approach to Successful Workovers in Karachaganak Gas Condensate Field. Paper SPE 81084 presented at the SPE Latin

American and Caribbean Petroleum Engineering Conference in Port-of-Spain, Trinidad, West Indies, 27-30 April.

Benesch, J., Gahr, J., Al-Mohsin, A., and Schmidt, M. (2007). Optimization of High-Pressure, High-Rate (HP/HR) Gas Wells in Giant Offshore Field. Paper SPE 105712 presented at 15th SPE Middle East Oil & Gas Show and Conference, Kingdom of Bahrain, 11-14 March.

Boom, W., Wit, K., Zeelenberg, J., Weeda, H., and Maas, J. (1996). On the Use of Model Experiments for Assessing Improved Gas-Condensate Mobility Under Near-Wellbore Flow Condition. Paper SPE 36714 presented at the SPE Annual Technical Conference and Exhibition, Denver, Colorado, 6-9 October.

Coats, Keith. (1982). Simulation of Gas Condensate Reservoir Performance. Paper SPE 10512 presented at the SPE Reservoir Simulation Symposium, New Orleans, Louisiana, 31 January-3 February.

Dacun, L., and Engler, T. (2001). Literature Review on Correlations of the Non Darcy Coefficient. Paper SPE 70015 presented at SPE Permian Basin Oil and Gas Recovery Conference, Midland, Texas, May.

Dake, L. (1978). *Fundamentals of Reservoir Engineering*. Amsterdam, The Netherlands: Elsevier.

Dehane, A., Algeria, D., and Osisanya, S. (2000). Comparison of the Performance of Vertical and Horizontal Wells in Gas-Condensate Reservoirs. Paper SPE 63164 presented at SPE Annual Technical conference and Exhibition, Dallas, Texas, 1-4 October.

El-Banbi, A., McCain, W., and Semmelbeck, M. (2000). Investigation of Well Productivity in Gas-Condensate Reservoirs. Paper SPE 59773 presented at SPE/CERI Gas Technology Symposium, Calgary, Alberta Canada, 3-5 April.

Elliott, S., Hsu, H., O'Hearn, T., Sylvester, I., and Vercesi, R. (1998). The Giant Karachagank Field, Unlocking its Potential. Oilfield Review. (Autumn 1998) 16-25.

Energy Information Administration, 2009, Natural Gas, http://www.eia.doe.gov/

Evans, R., Hudson, C., and Greenlee, J. (1985). The Effect of an Immobile Liquid Saturation on the Non Darcy Flow Coefficient in Porous Media. Paper SPE 4206 presented at the SPE Annual Technical Conference and Exhibition, Las Vegas, Nevada, 22-25 September.

Fahes, M., and Firoozabadi, A. (2005). Wettability Alteration to Intermediate Gas-Wetting in Gas/Condensate Reservoirs at High Temperatures. Paper SPE 96184 presented at SPE Annual Technical Conference and Exhibition, Dallas, Texas, 9-12 October.

Firoozabadi, A., Thomas, L., and Todd, B. (1992). High-Velocity Flow in Porous Media. Paper SPE 24869 presented at the SPE Annual Technical Conference and Exhibition, Washington, DC, 4-7 October.

Frederick, D., and Graves, R. (1994). New Correlations to Predict Non Darcy Flow Coefficients at Immobile and Mobile Water Saturation. Paper SPE 28451 presented at the SPE 69th Annual Technical Conference and Exhibition, New Orleans, Louisiana, 25-28 September.

Geertsma, J. (1959). Estimating the Coefficient of Inertial Resistance in Fluid Flow Through Porous Media. Paper SPE 4706 received in Society of Petroleum Engineers office in 1959.

Harisch, R., Bachman, R., Puchyr, P., and Strashok, G. (2001). Evaluation of a Horizontal Gas-Condensate Well Using Numerical Pressure Transient Analysis. Paper SPE 71588 presented at SPE Annual Technical Conference and Exhibition, New Orleans, Louisiana, 30 September-3 October.

Hashemi, A., and Gringarten, A. (2005). Comparison of Well Productivity Between Vertical, Horizontal and Hydraulically Fractured Wells in Gas-Condensate Reservoirs. Paper SPE 94178 presented at SPE Europe/EAGE Annual Conference, Madrid, Spain, 13-16 June.

Jones, S. (1987). Using the Inertial Coefficient, B, To Characterize Heterogeneity in Reservoir Rock. Paper SPE 16949 presented at 62nd Annual Technical Conference and Exhibition of the Society of Petroleum Engineers, Dallas, Texas, 27-30 September.

Khalaf, A. (1997). Prediction of Flow Units of the Khuff Gas Formation. Paper SPE 37739 presented at the SPE Middle East Oil Show, Kingdom of Bahrain, 15-18 March.

Kumar, V., Pope, G., and Sharma, M. (2006). Improving the Gas and Condensate Relative Permeability Using Chemical Treatments. Paper SPE 100529 presented at SPE Gas Technology Symposium, Calgary, Alberta, Canada, 15-17 May.

Lee, S., and Chaverra, M. (1998). Modelling and Interpretation of Condensate Banking for the Near Critical Cupiagua Field. Paper SPE 49265 presented at the SPE Annual Technical Conference and Exhibition, New Orleans, Louisiana, 27-30 September.

Li, K. and Firoozabadi, A. (June 2000). Phenomenological Modeling of Critical Condensate Saturation and Relative Permeabilities in Gas Condensate Systems, SPEJ **5** (2):138-147.

Li, K. and Firoozabadi, A. (April 2000). Experimental Study of Wettability Alteration to Preferential Gas-Wetting in Porous Media and Its Effects, SPEREE **3** (2):139-149.

Liu, X., Civan, F., and Evans, R. (1995). Correlation of the Non Darcy Flow Coefficient, J. Cdn. Pet. Tech., December, No. 10, 50-54.

Lohrenz, J., Bray, B., and Clark, C. (1964). Calculating Viscosities of Reservoir Fluids From Their Compositions. Paper SPE 915 presented at SPE Annual Fall Meeting, Houston, Texas, 11-14 October.

Martin, J. (1979). Cubic Equations of State-Which? Ind. Eng. Chem. Fundam. **18** (2): 81-97.

McCain, W. (1990). *The Properties of Petroleum Fluids*. Tulsa, Oklahoma: PennWell Publishing Company.

Muladi, A., Pinczewski, W. (1999). Application of Horizontal Well in Heterogeneity Gas Condensate Reservoir. Paper SPE 54351 presented at SPE Asia Pacific Oil and Gas Conference and Exhibition, Jakarta, Indonesia, 20-22 April.

Narayanaswamy, G. (1998*).* Well Productivity of Gas Condensate Reservoirs. MS Thesis, The University of Texas at Austin, Texas.

Panga, M., Ismail, S., Cheneviere, P., and Samuel, M. (2007). Preventive Treatment for Enhancing Water Removal From Gas Reservoirs by Wettability Alteration. Paper SPE 105367 presented at the 15th SPE Middle East Oil & Gas Show and Conference, Kingdom of Bahrain, 11-14 March.

Phipps, S., and Khalil, J. (1975). A Method for Determining the Exponent Value in a Forchheimer-Type Flow Equation. JPT Forum. Paper SPE 5325, July.

Pathak, P., Fidra, Y., Avida H., Kahar, Z., and Agnew, Mark. (2004). The Arun Gas Field in Indonesia: Resource Management of a Mature Field. Paper SPE 87042 presented at the SPE Asia Pacific Conference on Integrated Modeling for Asset Management, Kuala Lumpur, Malaysia, 29-30 March.

Rahman, O., and Al-Maslamani, M. (2004). GTL: Is it an Attractive Route for Gas Monetization? Paper SPE 88642 presented at the 11th Abu Dhabi International Petroleum Exhibition and Conference, Abu Dhabi, U.A.E., 10-13 October.

Schlumberger, 2009, Glossary, http://www.glossary.oilfield.slb.com

Tang, G., and Firoozabadi, A. (2000). Relative Permeability Modification in Gas/Liquid systems Through Wettability Alteration to Intermediate Gas Wetting. Paper SPE 81195 presented at SPE Annual Technical Conference and Exhibition, Dallas, 1-4 October.

Tek, M., Coats, K., and Katz, D. (1961). The Effect of Turbulence on Flow of Natural Gas Through Porous Reservoirs. Paper SPE 147 presented at SPE 36th Annual Fall Meeting, Dallas, Texas, 8-11 October.

Thauvin, F., and Mohanty, K. (1998). Network Modeling of Non Darcy Flow Through Porous Media, *Transport in Porous Media*, 31, pp. 19-37.

Whitson, C., and Kuntadi, A. (2005). Khuff Gas Condensate Development. Paper IPTC 10692 presented at International Petroleum Technology Conference, Doha, Qatar, November 21-23.

Wu, S., and Firoozabadi, A. (2009). Effect of Salinity on Wettability Alteration of Porous Media From Liquid Wetting to Intermediate Gas Wetting. Paper SPE 121724 presented at SPE International Symposium on Oilfield Chemistry, The Woodlands, Texas, USA, 20-22, April.

VITA

Name:	Nathan Miller
Address:	Harold Vance Department of Petroleum Engineering c/o Dr. Ding Zhu Texas A&M University 3116 TAMU-507 Richardson Building College Station, TX 77843-3116
Email Address:	nathan.miller@qatar.tamu.edu
Education:	B.S., Civil Engineering, Texas A&M University, 2007 M.S., Petroleum Engineering, Texas A&M University, 2009